

Recent Advances in Poly(*N*-isopropylacrylamide) Hydrogels and Derivatives as Promising Materials for Biomedical and Engineering Emerging Applications

Sonia Lanzalaco,* Júlia Mingot, Juan Torras, Carlos Alemán,* and Elaine Armelin*

Temperature-sensitive (thermosensitive) hydrogels, which are part of the family of stimulus-sensitive hydrogels, consist of water-filled polymer networks that display a temperature-dependent degree of swelling. Thermosensitive hydrogels, which can undergo phase transition or swell/de-swell as temperature changes, have great potential in various technological and biomedical purposes for a number of reasons: their temperature response is reversible, hydrogels are stable and easy to prepare, they can be biocompatible and also be suitably combined with other organic and inorganic materials, resulting in new materials with outstanding properties. Among thermosensitive hydrogels poly(*N*-isopropylacrylamide) (PNIPAAm) is the most extensively studied because it brings together the best properties of these materials. Consequently, in the past few years, a wide number of applications and new chemical processes to prepare PNIPAAm and their derivatives are being proposed. The objective of this review is to summarize the fundamentals of thermosensitive hydrogels and recent advances in preparation and both technological and biomedical applications of thermosensitive hydrogel, with a special focus on PNIPAAm and their derivatives. Special attention has been given to the discussion of challenges and future research perspectives based on new horizons not yet considered.

1. Introduction

Hydrogels play a significant role in the medical field as they provide enhanced performance as drug carriers for cell and gene therapies, tissue engineering, and 3D-printed artificial organs, due to their soft condition as polymeric material and high biocompatibility.^[1–4] Moreover, most of them are derived from biopolymers obtained by friendly and clinical-grade technology processes, such as bacterial fermentation and photosynthesis of plants and vegetables.^[5] Hydrogels are water-swollen crosslinked polymer networks, highly capable of absorbing water (up to 100 times its weight) without dissolving on it. They can be designed to act under different stimulus-responses.^[6,7] Stimuli-responsive materials change their properties upon exposure to one or more external induced changes, such as heat,


light, pH change, mechanical input, electrical input, chemical input, and magnetic input.^[8,9] Thermoresponsive or thermosensitive hydrogels (TSHs), i.e., gels with variable properties under temperature cooling or heating processes, have attracted much attention in the biomedical field.^[10,11] However, nowadays they are coming into force to be applied in other areas, among them, the very fascinating are those related to water waste treatments^[12–16] and energy production.^[17–20] Nowadays, one of the most promising gel-type polymers that are being explored in such emerging fields is poly(*N*-isopropylacrylamide) (PNIPAAm) and its copolymers. They can absorb (“expand”) or expel water (“collapse”) depending on the temperature of use and on the co-monomers class linked to the gel networking formation.

This review aims to offer a clear background in the TSH hydrogel concept with emphasis on the most relevant synthesis procedures and properties. Looking into the literature, over the past 5 years, more than 100 revisions about “thermosensitive” or “thermo-responsive” hydrogels were cited in the Web of Science. Among them, 58% were devoted to drug delivery and injectables,^[21–23] 16% was specifically related to gene and cancer therapy,^[24,25] 14% to tissue engineering,^[26–28] 4% to wound healing (dressing),^[29,30] 4% to the antimicrobial system^[31,32] and the rest appeals to other specific functions.^[33] Only five revision articles were inquired into other areas, such as agricultural^[34] and soft-robotics.^[35,36] The present work differs from

S. Lanzalaco, J. Mingot, J. Torras, C. Alemán, E. Armelin
Innovation in Materials and Molecular Engineering (IMEM)
Departament of Chemical Engineering
Universitat Politècnica de Catalunya (UPC)
C/ d'Eduard Maristany, 10-14 Building I, 2nd floor, 08019 Barcelona, Spain
E-mail: sonia.lanzalaco@upc.edu; carlos.aleman@upc.edu;
elaine.armelin@upc.edu

S. Lanzalaco, J. Mingot, J. Torras, C. Alemán, E. Armelin
Barcelona Research Centre for Multiscale Science and Engineering
Universitat Politècnica de Catalunya (UPC)
C/ d'Eduard Maristany, 10-14, Building I, basement, 08019 Barcelona, Spain

C. Alemán
Institute for Bioengineering of Catalonia (IBEC)
The Barcelona Institute of Science and Technology
C/ Baldiri Reixac 10-12, 08028 Barcelona, Spain

 The ORCID identification number(s) for the author(s) of this article can be found under <https://doi.org/10.1002/adem.202201303>.

© 2022 The Authors. Advanced Engineering Materials published by Wiley-VCH GmbH. This is an open access article under the terms of the Creative Commons Attribution-NonCommercial-NoDerivs License, which permits use and distribution in any medium, provided the original work is properly cited, the use is non-commercial and no modifications or adaptations are made.

DOI: 10.1002/adem.202201303

those previously published on the topic, being set on the novelty of exploring new horizons, with a particular focus on PNIPAAm (and derivatives) TSHs uses.

2. Basic Features

2.1. Hydrogel Concept and General Properties

Hydrogels were first reported by Wichterle and Lím in 1960.^[37] The original hydrogel polymer was composed of a copolymer of 2-hydroxyethyl methacrylate (HEMA) and ethylene dimethacrylate (EDMA). Thus, derived from synthetic sources. One year later, it was converted into the first soft hydrogel successfully used as contact lenses, which remains one of the most important clinical uses of hydrogels today.

According to polymers' nature and their combinations with other organic and inorganic compounds, hydrogels can be classified as shown in **Figure 1**. Although the most important class refers to natural and synthetic groups, natural-based hydrogels are the most abundant.^[38] Combinations of either natural or synthetic gels with other materials (e.g., ceramic, metallic, and living organisms) derive in hybrid systems. **Table 1** includes examples of polysaccharides, synthetic and hybrid gel types, with particular emphasis on that which describes their thermoresponsive properties. Many of these examples are combinations of different hydrogel-like structures, such as poly(*N*-isopropylacrylamide) (PNIPAAm) with natural gel compounds. PNIPAAm is one of the most important synthetic thermosensitive hydrogels investigated nowadays.

A hydrogel is a 3D network of hydrophilic polymers that can swell in water and hold a large amount of it, while maintaining the structure due to chemical or physical crosslinking of individual polymer chains (**Figure 2**). One example of natural- and synthetic hydrogel interactions by hydrogen bonds to form cellulose–polyacrylamide interpenetrating network was shown by Lin et al.^[39] The high swelling/de-swelling capacity under environment changes will depend on both the chemical structure of the polymer structure and the degree of crosslinking. Such entanglement linkages are responsible for the high porosity of these compounds.

The most important natural, synthetic, and hybrid TSHs are described in the next section, highlighting their relevant properties and applications.

2.2. Chemical Structures and Properties of Most Relevant Thermosensitive Hydrogels

TSHs have received considerable attention in the past decades,^[40,41] because they undergo an in situ sol–gel transition at values of temperature which could correspond to the difference in their ambient storage temperature and their critical solution temperature (CST). TSHs only form gels once a change in the hydrophilic and hydrophobic interactions, among the polymer chains and the water molecules making up the solution, is induced.^[42] It is possible to define a lower critical solution temperature (LCST) when polymers gel, upon heating, moves from soluble and hydrophilic to insoluble and hydrophobic.^[43] Conversely, when the sol–gel transition occurs upon cooling,

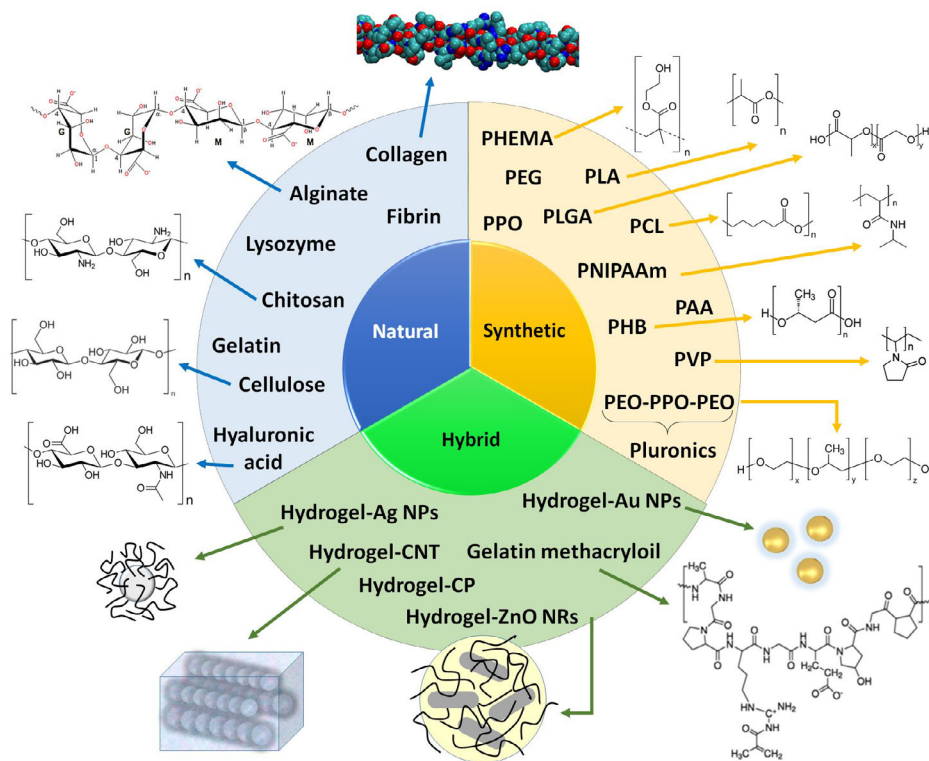


Figure 1. Hydrogel classification according to polymer nature and combinations of them with other organic and inorganic compounds.

Table 1. Main examples of TSH hydrogels, classified according to their polymer nature and main applications.

Hydrogel nature	Main properties and/or applications	References
Alginate/Ploxamer 407	Dental caries treatment	[192]
Alginate/sodium hyaluronate/ methylcellulose composite	Arthritis treatment	[193]
Alginate/PNIPAAm	Recovery of Li from seawater	[187]
Alginate/PNIPAAm/ ϵ -polylysine	Recovery of uranium from seawater	[188]
Alginate/gelatin/ZnO	Scaffold for cartilage tissue regeneration	[194]
Chitosan	Injectable, controllable degradation, and drug delivery	[195]
Chitosan/alginate	Injectable hydrogels for ocular disease treatments	[196]
Hyaluronic acid/dextran		
PNIPAAm, PEG, PLGA		
Chitosan/PNIPAAm	Delivery of therapeutic proteins for cardiac protection against myocardial infarction	[197]
Methylcellulose	Oral dosage drug	[198,199]
	Prevention of post-operative adhesion	
Hydroxypropyl cellulose/ Konjac glucomannan biomass	Super hygroscopic collector of water from atmospheric moisture	[200]
Methacrylate gelatin	Adhesion, wound repair	[201]
Gelatin/silk	Nerve guidance conducts for nerve regeneration	[202]
Cellulose/Pluronic F127	Injectable drug delivery	[203]
PNIPAAm	Solar water evaporation	[164]
PNIPAAm-poly(acrylic acid) (PAA) copolymers	Smart window for building energy efficiency	[204,205]
	Artificial breathing actuator	
PEG-PCL copolymers	Injectable gel to deliver therapeutic proteins for ocular diseases	[68,206]
	Drug delivery, graft	
Poly(3-hydroxybutyrate) (PHB)	Tissue engineering	[207]
Hydrogel-Ag NPs	Antibacterial hydrogel for wound healing	[115,208,209]
	Antibacterial coating	
Hydrogel-Au NPs	Anticancer therapy	[101,106,107,132,133]
	Photothermal therapy and drug delivery	
	SERS detection, semi-invasive diagnosis	
Hydrogel-carbon nanotubes (CNT)	Absorbent for oil/water separation	[210,211]
	Drug delivery controlled by electrical and temperature stimulus	
Hydrogel-conducting polymers (CP)	Electrochemical sensor for herbicide detection	[103–105]
	Tissue engineering scaffolds, implantable biosensors	
	Self-healing properties	

they display an upper critical solution temperature (UCST). Another important parameter of the TSHs is the critical gelation concentration (CGC) which is defined as the concentration of a material that results in thermo-gelation, which affect the viscosity and the gelation temperature.^[43] Furthermore, the hybridization of TSHs with other materials has allowed researchers to formulate ideal TSHs to suit their requirements, thereby mitigating issues arising when the gelation concentrations are too high, or the gelation temperatures are not viable for in situ gelation.^[44] Key TSHs of great interest are chitosan- β -glycerophosphate, pluronic F127, methylcellulose (MC), poly(ethylene glycol)-block-poly(ϵ -caprolactone) (PEG-PCL)-based polymersomes and PNIPAAm. In the current review, special focus will be directed

to PNIPAAm and PNIPAAm-based hybrid TSHs, suitable for many applications in various processes ranging from industrial to biological.

2.2.1. Chitosan-Based Thermosensitive Hydrogels

Consisting of *N*-acetyl-D-glucosamine and β (1-4)-linked D-glucosamine randomly arranged, chitosan is a biodegradable, biocompatible, cationic polysaccharide that is hydrophilic and that can gel at body temperature when the pH is increased to 7.2.^[45] In 2001, Chenite et al. developed for the first time a chitosan-based thermogel causing the gelation by the addition of

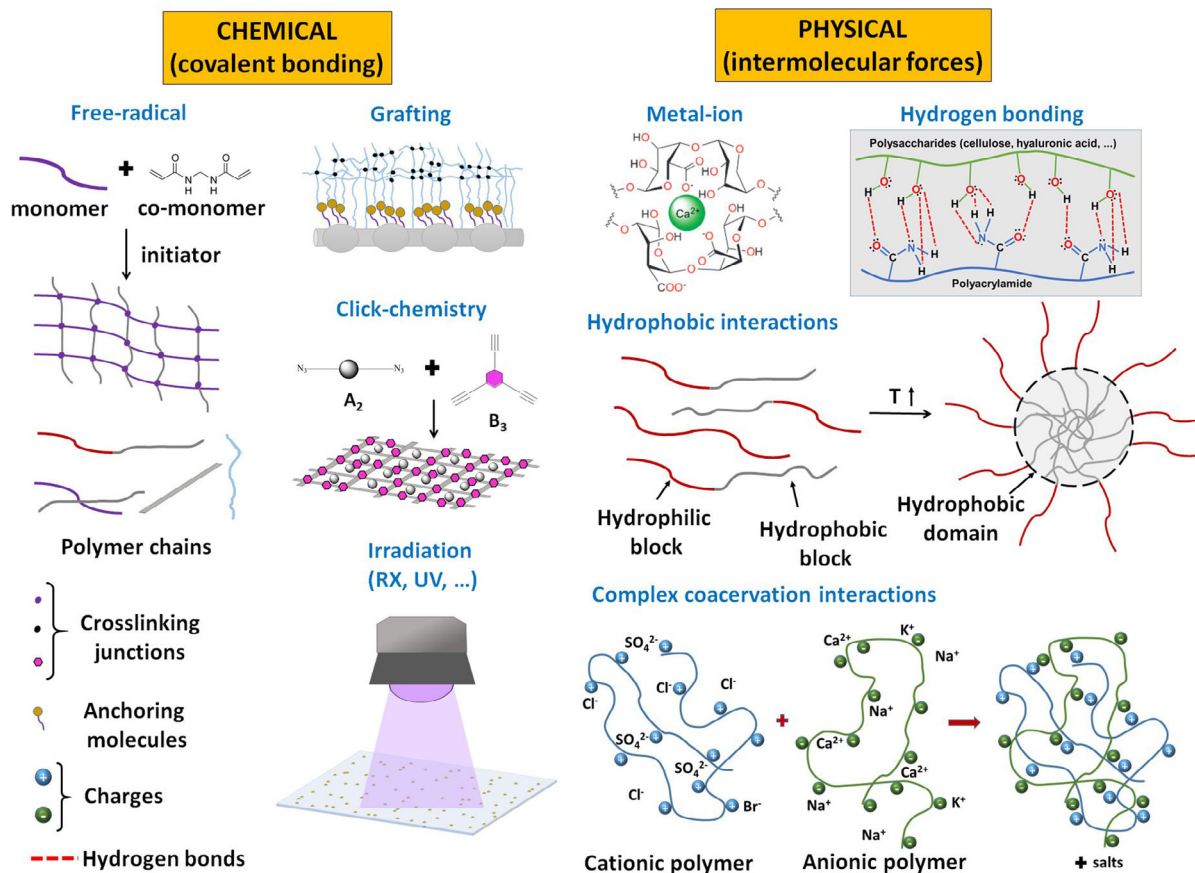


Figure 2. Chemical and physical examples of hydrogel crosslinking. Adapted from several references reported in the literature. Reproduced with permissions: Hydrogen bonding image.^[39] Copyright 2018, Springer Nature; Grafting image.^[133] Copyright 2022, American Chemical Society; Free-radical and crosslinking junctions.^[139] Copyright 2018, American Chemical Society; Metal-ion image.^[190] Copyright 2017, American Chemical Society; Click-chemistry image.^[191] Copyright 2017, American Chemical Society.

β -glycerophosphate, a polyol salt, that serves to increase the pH of the acidic chitosan to 7–7.4, allowing a gel to form in a controlled manner at 37 °C, while maintaining its liquid state at 10 °C.^[46] As regards the mechanism, the polyols surround the chitosan and provide a protective and hydro-resistant layer around the chitosan chains through weak intermolecular interactions such as hydrogen bonding. Increasing the temperature eliminates this polyol layer and allows the polymer to be in equilibrium through stronger hydrophobic interactions, thereby generating gels (Figure 3a).^[47,48] Hybrid chitosan-based TSHs show promising perspectives in terms of their potential in tissue engineering applications due to the reduction in toxicity and improvement in gel strength provided by hybridization with other compounds.^[2,49] An interesting study about the preparation and cell viability of hydrogel scaffolds based on chitosan, β -glycerophosphate, and collagen was reported by Song et al.^[50] The study revealed improvements in cell growth and in the performance of the chitosan/ β -glycerophosphate/collagen hybrid material. The formulation, which gelled within 12 min at a temperature of 37 °C, showed good mechanical strength and was able to maintain its integrity within the cell culture media for the entire duration of 4 weeks.^[50] A chitosan-PNIPAAm TSHs was formulated by Luo et al. for the treatment of oral

mucosal ulcers, with thermo-gelling temperatures ranging from 30.1 to 31.8 °C, thereby facilitating the injection within the oral cavity.^[51] The combination of chitosan and PNIPAAm led to an improvement in antimicrobial activity, inhibiting both Gram-positive and Gram-negative bacterial growth and promoting gingival fibroblast proliferation and the healing of ulcers.^[51]

2.2.2. Pluronic-Based Thermosensitive Hydrogels

Another class of TSHs is represented by pluronic (commonly known as poloxamer), triblock copolymers consisting of hydrophobic polypropylene oxide (PPO) at the center, with hydrophilic polyethylene oxide (PEO) on either sides (ABA poloxamer), whose precise mechanism of gelation has not been yet confirmed.^[52] Different hypotheses have been proposed during the past decades,^[53,54] most of them based on changes in the properties of the micelles with regards to aggregation and symmetry upon an increase in temperature.^[53] In all models investigated, the increasing temperature caused the gelation, leading to the formation of the micelles from unimers (at low temperature) and, subsequently, to the formation of entanglements between the micelles.^[55,56] The entanglements could be ascribed to a shortening of the intermicellar distance that takes place by

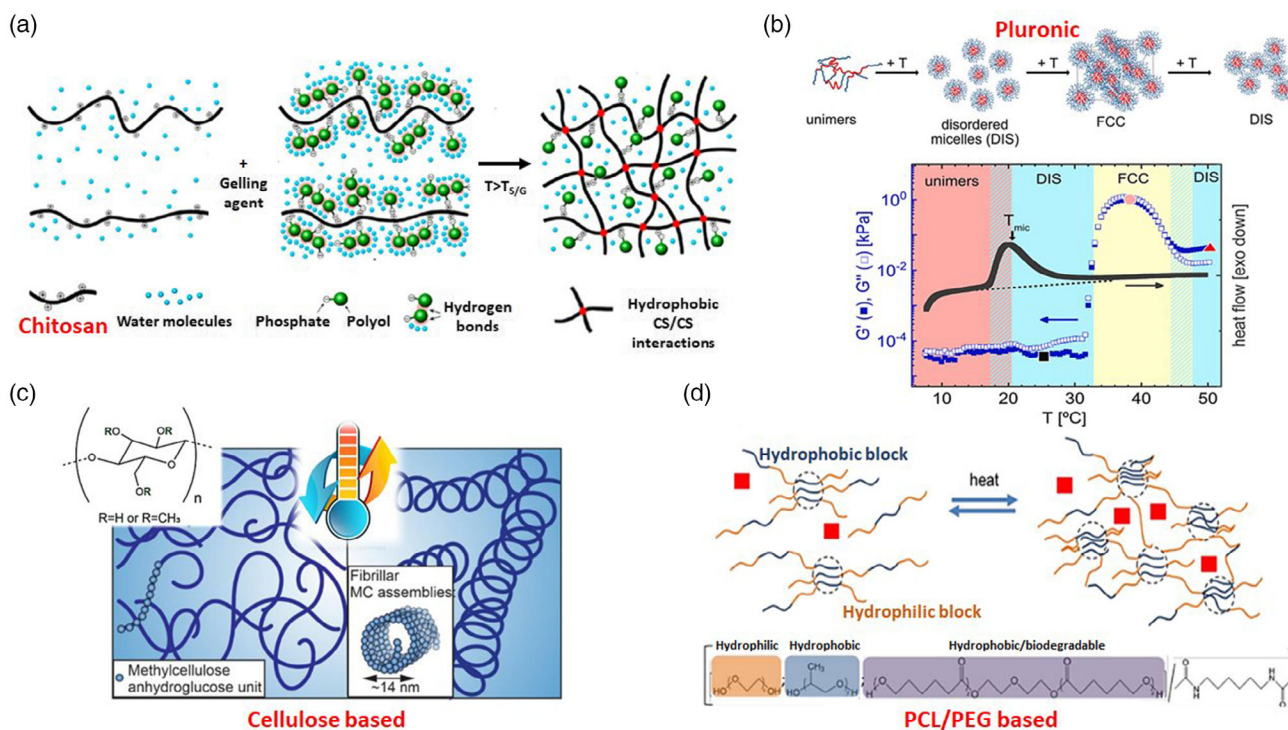


Figure 3. a) Schematic representation of gelation mechanism of thermal-sensitive chitosan/polyol-phosphate systems. Reproduced with permission.^[47] Copyright 2013, American Chemical Society. b) Aqueous 15% w/v P407 micelles with increasing temperature, as is shown by the endothermic differential scanning calorimetry (DSC) peak (black curve). Micelles are disordered at 25 °C. With further temperature elevation, a sharp increase in G' and G'' is observed as the micelles pack into FCC structures (pink dot). In the aforementioned physiologically relevant conditions, the moduli decrease as the micelles disorder (DIS, red triangle). Reproduced with permission.^[56] Copyright 2022, Elsevier. c) The chemical structure of MC. At 20 °C (left side), aqueous MC behaves as individual polymer chains, while at 60 °C (right side), the aqueous MC chains are supramolecularly aggregated into shape-persistent fibrils with hollow ring-like lateral structure. Reproduced with permission.^[64] Copyright 2018, American Chemical Society. d) Thermogelling poly(PEG-PPG-PCL-urethane) copolymer for protein delivery. Upon heating, the multiblock copolymer is able to generate crosslinks and form a hydrogel under mild conditions to encapsulate protein drug. Reproduced with permission.^[68] Copyright 2019, Royal Society of Chemistry.

increasing the micellar sizes or the micelles numbers. As a model, a recently published mechanistic study of one of the most commonly used pluronic, F127, also known as poloxamer 407 (P407), has been reported. Figure 3b shows the formation of aqueous P407 micelles with increasing temperature. With further temperature elevation, micelles packed into FCC structures at 37 °C, as revealed by a sharp increase in G' and G'' curves. Above physiologically relevant conditions, the moduli decrease as the micelles disorder. In the same study, it was also investigated the impact of adding to P407 2 BAB reverse poloxamers (RPs), 25R4 and 31R1, on the thermal transitions, rheological properties, and mainly on the assembled structures of P407 was also investigated.^[56] While 25R4 addition promotes inter-micelle bridge formation, the highly hydrophobic 31R1 co-micellizes with P407. Small molecule addition reduces the thermal transition temperatures and increases the micelle size, while RPs addition mitigates the decreases in modulus traditionally associated with small molecule incorporation.^[56] The high CGC of P407, which is a triblock copolymer with a 2:1 PEO:PPO ratio, is a serious disadvantage.^[57] This value, which was found to be greater than 20% at 25 °C, is responsible for the formation of gels with high viscosity, not suitable for many applications (i.e., drug injection^[57]). To mitigate such drawback, some authors proposed hybridization of P407 with MC, lowering the

CGC to 12% and showing a thermo-gelation at 37 °C while existing in the sol phase at room temperature.^[57] Also, pluronic was efficiently hybridized with alginate (ALG). The mechanical properties of the thermo-gelling system improved around 100 times.^[58] Furthermore, ALG addition led to an increase in the temperature from 15 to 40 °C, indicating higher stiffness of the gel.^[58]

2.2.3. Cellulose-Based Thermosensitive Hydrogels

MC and hydroxypropyl methylcellulose (HPMC) are hydrophobically substituted water-soluble cellulose derivatives that are thermoresponsive with an LCST comprised between 40 and 50 °C and between 75 and 90 °C for MC, and HPMC, respectively.^[59] At concentrations between 1% and 10%, these polymers form gels at a temperature higher than the LCST. Several mechanisms have been proposed to explain the thermo-reversible gelation of MC.^[60–62] One of the most recent, which was reported by Niemczyk-Soczynska et al.,^[61] can be described as follows. During heating, MC displays endothermic behavior, with an exothermic effect preceding this for MC concentrations below 2%. Raising from ambient temperature up to the LCST value, changes in the hydrophilic interactions among water molecules themselves and among water molecules and MC, followed by the

formation of methoxy groups and “water cages” (with water molecules surrounding the hydrophobic areas of MC) were observed. Finally, intra- and intermolecular hydrophobic interactions result in the crosslinking of the methoxy group within the MC chains and this is known as the high-temperature endothermic effect.^[61] Very interestingly, as a result of the heating, MC chains in aqueous solutions aggregate into persistent fibrils with a hollow ring-like lateral structure of ≈ 14 nm diameter and length of several hundreds of nm, while at room temperature MC chains exist in the form of random coils (Figure 3c).^[63,64]

Due to the high gelation temperature of cellulose-based TSHs, modification of these polymers has been carried out to reach temperatures close to the physiological. Actually, it is possible to decrease the gelation temperature by increasing the concentration of MC, even though this modification results in an increase in the viscosity. Alternatively, a salt could be added. Encouraging results in reducing the gelation temperature of MC to 32 °C and, simultaneously, speeding up the gelation process were obtained by adding xylitol and sodium phosphate dibasic. Furthermore, the addition of polyethylene glycol (PEG) to this system increased the rate of gelation from 20 min to a mere 150 s.^[60] The authors demonstrated good blood flow after hydrogel injection in rats (in vivo), enhanced neovascularization and improved inhibition of muscle atrophy. In contrast, the blending of calcium chloride and ALG with MC resulted in the formation of a crosslinked and strong gel after 10 min at 37 °C, which was used as an injectable medium for the delivery of chitosan microparticles.^[65] Then, the low toxicity of cellulose-derived TSHs deserves potential application of this polysaccharide in the biomedical field.

2.2.4. PCL-PEG-Based Thermosensitive Hydrogels

The hydrophobic, biodegradable, and biocompatible poly(ϵ -caprolactone) (PCL) could be combined with the hydrophilic PEG in the formation of di- and triblock copolymers, such as PEG-PCL-PEG and PCL-PEG-PCL, which can be reconstituted into TSHs.^[66,67] The structure and mechanism of thermogelation of poly(PEG-PPG-PCL-urethane)-based TSHs are shown in Figure 3d. Upon heating, the multiblock copolymer is able to generate crosslinks and form a hydrogel under mild conditions and to encapsulate protein drug.^[68] Poly(PEG-PPG-PCL-urethane) thermo-gelling systems, where PPG refers to polypropylene glycol, were obtained by hybridizing PEG-PCL-based TSHs and optimized to improve the release profile of paclitaxel in the treatment of tumors.^[68] The resulting solution formed a gel with excellent mechanical properties. Furthermore, poly(PEG-PPG-PCL-urethane) TSHs have been used to deliver anti-vascular endothelial growth factor proteins, inhibiting angiogenesis and mitigating the need for multiple injections.^[68] The best release profile for this application was obtained by altering the hydrophilic/lipophilic balance through the PEG:PPG ratio (4:1). Such study, which was conducted both ex vivo and in vivo, represented a steppingstone for the development and use of TSHs in the delivery of bioactive protein molecules.^[68]

The solubility and temperature responsiveness of PEG-PCL-based TSHs was improved by Oroojalian et al. through the synthesis of a mPEG-*b*-[PCL-*g*-(MEO₂MA-*co*-OEGMA)]-*b*-mPEG block graft copolymer.^[69] Because of the hydrogen bonds formed

between water molecules and the hydrophilic oligo(ethylene glycol) graft, the synthesized copolymer showed better solubility in water. A 3D and interconnected structure, similar to that of the extracellular matrix, was obtained through the hybridization of PEG-PCL with PNIPAAm, resulting in a penta-block PNIPAAm-PCL-PEG-PCL-PNIPAAm TSH for application in wound healing.^[70] Such formulation displayed excellent biocompatibility and was able to gel at 37 °C, its pore size being ideal for fibroblast attachment as well as for the improvement of cell adhesion and proliferation.^[70]

The focus of this review is driven by PNIPAAm hydrogel and its derivatives. Therefore, a detailed description of its chemical structure and relationship with the LCST transition, synthesis, and main properties are provided in the following sections.

3. Poly(*N*-isopropylacrylamide) Based Thermosensitive Hydrogels

3.1. Basic Features

PNIPAAm has attracted a lot of attention during the past decades because of its thermo-responsive behavior in a biomedical interesting temperature window.^[10] PNIPAAm is a synthetic thermo-responsive polymer obtained from an acrylamide monomer, *N*-isopropylacrylamide (NIPAAm), composed of amide and propyl groups.^[71] The thermal behavior of PNIPAAm in aqueous media consists of a phase transition from a hydrophilic state to a hydrophobic one when it is heated above its LCST.^[72] Thus, as long as the temperature of the hydrogel is lower than LCST, it can absorb water and swell, but once LCST is exceeded, the PNIPAAm network will collapse and precipitate.^[71,73]

Water molecules form hydrogen bonds with the carbonyl group, accepting two hydrogen bonds, and the nitrogen atom of the amide group can donate one hydrogen bond in the hydrated state below LCST (Figure 4a). When the LCST temperature is exceeded, rearrangement of intramolecular hydrogen bonds occurs. During this transition, it has been shown that the number of hydrogen bonds between PNIPAAm and water is reduced and intra-chain hydrogen bonds are formed.^[74] It is the reason for the formation of the collapsed network of PNIPAAm chains above LCST (Figure 4b). However, the mechanism followed by PNIPAAm to self-assemble in water above the LCST is not fully understood. Another explanation considers that the enthalpy gain of water molecules associated via hydrogen bonds with the amide groups of the polymer becomes smaller than the counter effect of entropic gain of the system with water being dissociated when above the LCST of the hydrogel.^[75] Furthermore, computer simulations showed that besides a reduction of intermolecular hydrogen bonds, there is a substantial decrease in the solvent-accessible surface area, and it has been even suggested that a decrease in torsional energy of the isopropyl groups occurs during this thermal transition.^[76]

3.2. Synthesis of Poly(*N*-isopropylacrylamide) Hydrogels

Commonly, PNIPAAm is synthesized in solution by free-radical polymerization (FRP) using NIPAAm as a monomer, a cross-linker, and an initiator to trigger the reaction. The physical

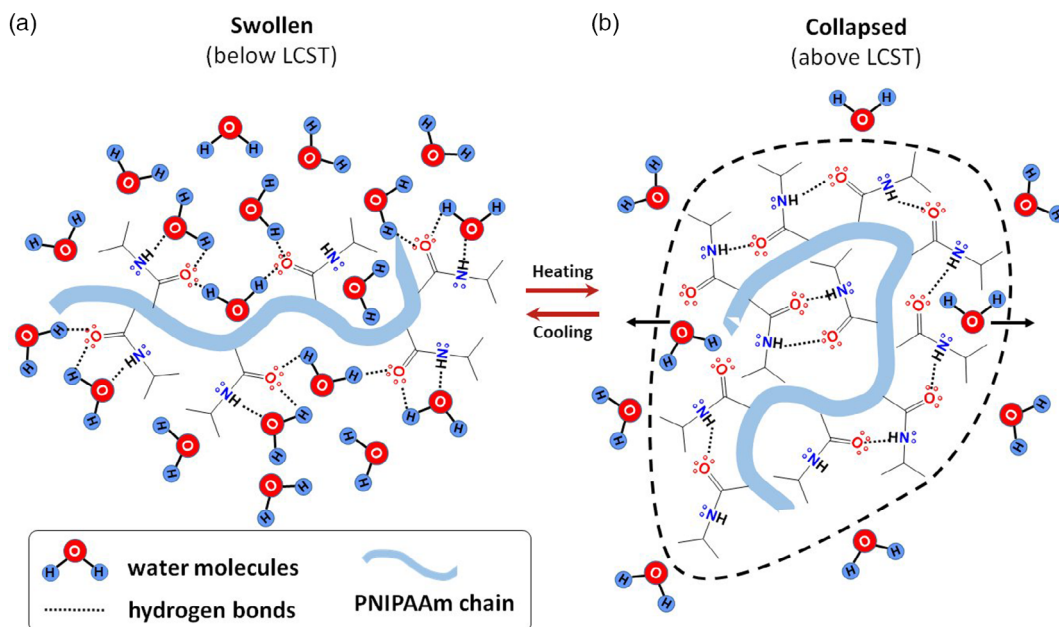


Figure 4. Schematic representation of: a) water swelling and b) de-swelling mechanisms of PNIPAAm chains, induced by lower critical solution temperature (LCST) temperature changes, and hydrogen bonding formations.

and chemical properties of the synthesized hydrogels can vary depending on the type, proportion, and concentration of these elements in the reaction sample.^[77] The main property is the already mentioned temperature sensitivity. Although for PNIPAAm hydrogels the phase change is considered to occur at 32 °C, such LCST varies.

FRP and controlled living radical polymerization (LRP) are the most used procedures for the synthesis of PNIPAAm hydrogels.

3.2.1. Free-Radical Polymerization

This consists of polymerizing the hydrophilic NIPAAm monomer, which is commercially available, with small amounts of cross-linking agents (MBA, *N,N'*-methylene bis(acrylamide)) (Figure 5).^[78] To initiate the reaction, the initiator (APS, ammonium persulfate) is decomposed into free radicals, either heating

or irradiating with UV. Free radicals react with the unsaturated carbon—carbon bonds (C=C) of the monomers, thus propagating the chain until termination occurs (two molecules with free radicals react with each other).^[79] *N,N,N',N'*-tetramethylethylenediamine (TEMED) is usually used as a catalyst to accelerate the radical polymerization.

This method has several disadvantages, including difficulties in controlling the particle size, polydispersity, degree of polymerization, or polymer microstructure. However, its advantages include the ease of controlling the reaction conditions, the possibility of using a wide variety of monomers, and the use of both aqueous and organic solvents (the most commonly used being methanol, benzene, and acetone).^[10] Ziminska et al. obtained a biodegradable thermosensitive hydrogel for sustained drug release using chitosan and NIPAAm. The hydrogel, which was stable at the physiological temperature, was prepared using APS as the initiator and TEMED as the accelerator.^[80]

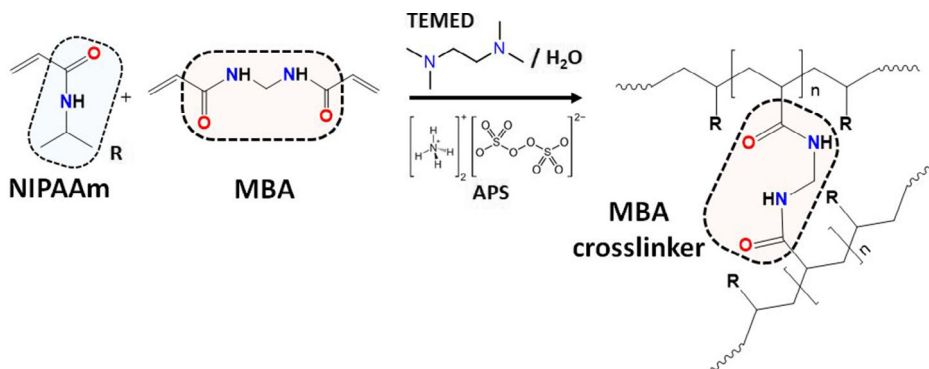


Figure 5. Synthesis of PNIPAAm hydrogel crosslinked with MBA crosslinker.

3.2.2. Controlled LRP

Live radical polymerization differs from FRP in the fact that the radical lifetime in the propagation stage is longer, allowing to control the polymer molecular weight, architecture, and composition. The main characteristics of this kind of polymerization are fast initiation, slow propagation, and no termination.^[79]

Atom transfer radical polymerization (ATRP) is a controlled living radical copolymerization that allows control of reaction kinetics, molecular weight distribution (low dispersion), and regulation of complex molecular architectures. Moreover, the ATRP of NIPAAm can be carried out in both organic solvents and aqueous media. However, the ATRP of acrylamides can be problematic.^[79] Matyjaszewski et al.^[81,82] reported controlled living radical polymerization of some functional (metha)acrylamides by ATRP. However, it is known that generally NIPAAm polymerization cannot be properly controlled by ATRP, reversible addition-fragmentation radical polymerization, or cationic polymerization, but rather by reversible atom fragmentation transition (RAFT) polymerization.^[83]

The difference between RAFT polymerization compared to ATRP is that it does not require a metal catalyst but a radical initiator and a RAFT chain transfer agent (CTA).^[79] Benefits of RAFT polymerization include obtaining (co)polymers with a controlled molecular weight and narrow distribution.^[83] Appropriate choice of the CTA is crucial to achieving well-controlled RAFT polymerization of NIPAAm.^[84]

3.2.3. Graft Copolymerization

Different methods for the graft copolymerization of PNIPAAm have been described: hydrogel copolymer grafted onto solid surfaces; photo-induced grafting copolymerization; plasma-induced grafting copolymerization; irradiation copolymerization.^[85,86]

Regarding the medium, solution and bulk polymerizations are applied for homogeneous phases while emulsion polymerization is performed for heterogeneous phases. PNIPAAm hydrogels obtained using the first two methods exhibit random particle size distribution, whereas the last method allows to modulate the size from micro- to nanoscale.^[10]

Lanzalaco and coworkers developed a procedure to activate the surface of polypropylene (PP) meshes with oxygen-plasma and subsequent covalent graft of PNIPAAm-co-MBA hydrogel onto this surface.^[87] The complete mechanism is exemplified in **Figure 6**. The first step consists of PP mesh activation by cold-plasma treatment, followed by a subsequent immersion of the substrate in the mixture solution (second step), composed of NIPAAm monomer, MBA crosslinker, and peroxide activator (APS) for the radical polymerization. Afterward, the hydrogel covalent bonds are created at the activated surface of the PP fibers, with further growth among them. Finally, the PP/gel bilayer is removed from the reaction media (fourth step), washed, and neutralized to pH 7 to obtain the best gel grafting yield. The bilayer system was used to convert the inanimate PP surface into a temperature-responsive implant able to adapt to local temperature and humidity variations.^[88,89]

3.3. Physicochemical Properties Variations of Poly(*N*-isopropylacrylamide) Thermosensitive Hydrogel

3.3.1. Effect of Molecular Weight

Depending on the molecular weight, LCST of PNIPAAm may remain unchanged, increase or decrease.^[90–92] According to Furryk et al., the influence of the molecular weight and polydispersity of PNIPAAm on LCST is not significant when the molecular weight is above 50 kDa. Instead, the LCST varies for smaller polymers and is related to the presence of hydrophilic or hydrophobic end groups that cause LCST to increase or decrease, respectively.^[93] Furthermore, a content higher of 40 wt% of PNIPAAm, dissolved in water, causes a slight enhancement of the LCST value of only 1.5 °C. Even though a wide variation range of PNIPAAm content was investigated (5–60 wt%), the variability on LCST is not very noticeable, 3–3.5 °C between 28.5 and 32 °C only.^[80,94,95] Thus, when a much higher LCST temperature is desirable, NIPAAm monomer is copolymerized with other co-monomers to modulate such temperature. Copolymers of PNIPAAm will be introduced in the following sections.

3.3.2. Effect of Water/Organic Solvent Mixtures

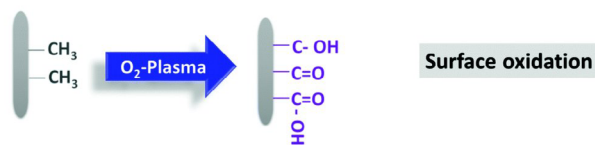
In water/organic solvent combinations, the LCST depends on the co-solvent volume fraction and its type. As a general rule, when the volume fraction of organic solvent increases, the LCST decreases, while when a certain volume ratio is reached, the LCST increases. At low volume ratios, the LCST decreases and it could be explained by the lack of hydration of PNIPAAm resulting from a competition for water molecules between PNIPAAm chains and the co-solvent molecules. The less polar the co-solvent, the lower the volume fraction at which the LCST increases.^[80] Moreover, the use of mixed solvents also improves the response dynamics rate, as typically, such response rate to external temperature changes is relatively slow, restricting PNIPAAm hydrogel applications.^[71]

Rana et al. studied the effect of the solvent polarity on PNIPAAm properties showing that, while the thermoresponsive behavior remains the same, both the microstructure and mechanical properties can be modulated.^[77] Microgels synthesized using nonpolar solvents display larger pore size and particle size (**Figure 7**), as well as higher swelling ratios.^[77] Experimental conditions can be modified to tune the properties of the synthesized hydrogels. For example, the improved surface hydrogel was obtained by polymerizing in gelled corn starch aqueous solution.^[96]

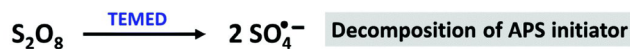
3.3.3. Effect of Copolymerization

The LCST of PNIPAAm hydrogel can be tuned by copolymerizing with more hydrophilic or hydrophobic monomers, as mentioned previously. Copolymerization with more hydrophilic monomers usually increases the LCST, while the opposite effect is observed upon the addition of more hydrophobic monomers.^[79] Copolymerization-induced regulation of the LCST is due to changes in the overall hydrophilicity of the polymer

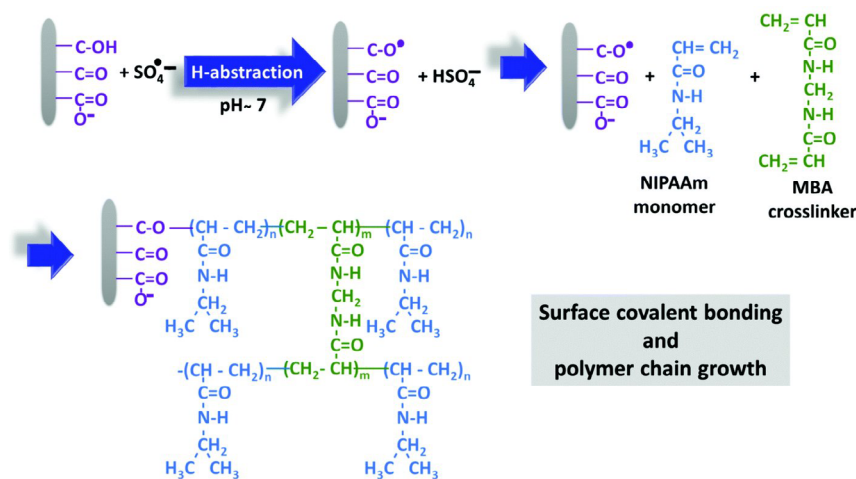
1st step: Surface functionalization by O₂-plasma treatment



2nd step: radical polymerization of NIPAAm-co-MBA under APS activation



3rd step: Grafting of NIPAAm onto plasma treated Optilene[®] mesh



4th step: H₃O⁺ formation



**Purification
and
neutralisation**

Figure 6. Illustration of the reaction mechanism involved in the PNIPAAm hydrogel deposition in PP fibers of hernia repair meshes, promoted by the exposure of its surface to oxygen plasma discharge. The PP fibers are represented by the grey perpendicular bar with CH₃ lateral groups and further conversion of them into polar groups, after the plasma attack. Reproduced with permission.^[87] Copyright 2019, Royal Society of Chemistry.

and, consequently, changes in the hydrogen bonding interactions with water molecules.^[97] For example, when combined with acrylamide monomers (AAm), the PNIPAAm LCST reaches about 37 °C, whereas if combined with hydroxyethylacrylamide (HEAm), with higher hydrophilicity, the LCST could increase up to 50 °C.^[98]

PNIPAAm hydrogels synthesized by free radical polymerization have poor mechanical properties^[99] (i.e., low elastic modulus, low yield strength, and shear stress) and poor biodegradability, affecting their applicability. However, copolymerization is among the different approaches used to improve mechanical properties.^[99] Copolymerization with natural polymers has also been demonstrated to be a challenge to potentiate the biodegradability of PNIPAAm-based hydrogels.^[10]

3.4. Hybrid Materials Derived from Acrylamide Thermosensitive Hydrogels

Nowadays, TSHs have been combined with other compounds, such as carbon nanotubes (CNT),^[100] metal nanoparticles,^[101,102] conducting polymers (CPs),^[103–105] and others, taking

advantages of the individual properties of such components and achieving new performances (e.g., soft robotics, drug delivery, diagnostic and bioimaging, sensors, among others). For instance, in the biomedical field, the combination of plasmonic nanoparticles with hydrogels has gained force due to their applicability in photothermal therapy. Wu et al.^[101] successfully reduced the cavity of resected cancerous breasts of rats by injecting poly(*N*-acryloyl glycinamide-*co*-acrylamide) hydrogel bearing polydopamine coated-gold nanoparticles (AuNPs) and charged with doxorubicin (DOX), an anticancer drug. The amount of released drug and the regeneration of the mammalian tissue were simultaneously regulated by applying controlled near-infrared (NIR) light for 4 weeks. Thus, the TSH actuated as both a drug carrier and a mammoplasty filler. Bong and coworkers^[106] also applied NIR light to efficiently deliver DOX in human cervical cancer HeLa cells. In this case, microparticles made of poly(*N*-vinylcaprolactam) and gold nanorods (AuNRs) were the drug carrier. In another example, Matai et al.^[107] designed a robust hydrogel patch to kill cancer cells under NIR irradiation. Such TSH was a hybrid system composed of a disk-shaped ALG/PAAm hydrogel, which contained

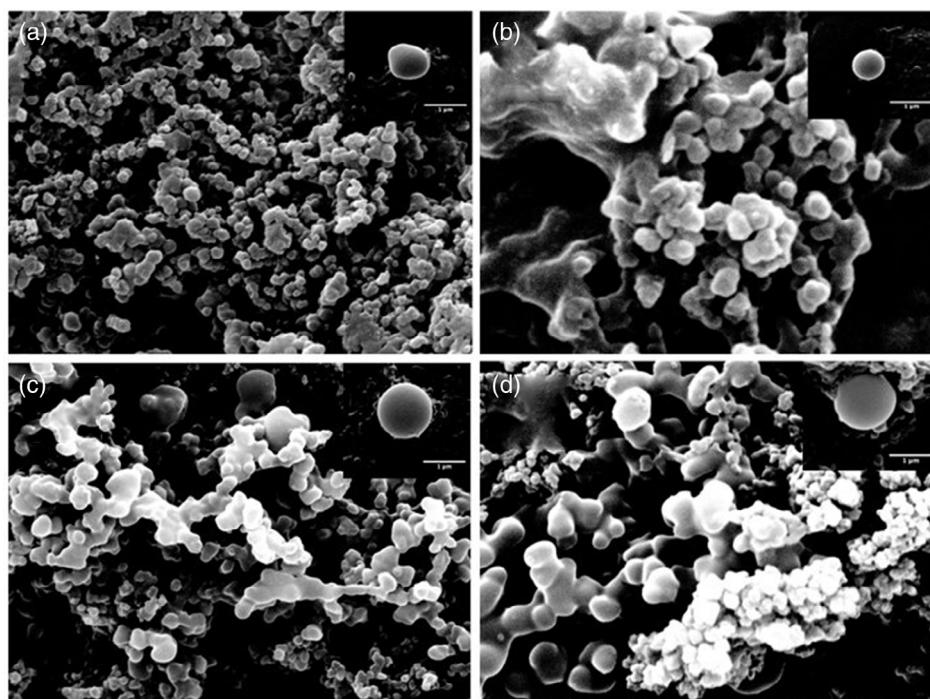


Figure 7. SEM micrographs of dispersed PNIPAAm microgels synthesized from: a) dioxane; b) THF; c) toluene; d) cyclohexane. Although microgels are spherical in all cases, they differ in size (scale bar: 1 μm). Reproduced with permission.^[77] Copyright 2021, Elsevier.

nanosheets of poly(vinylpyrrolidone) (PVP)-graphene oxide-AuNRs (PVP-nGO@AuNRs), and loaded with methotrexate (MTX) and rhodamine B (RhB), a chemotherapeutic drug and a dye, respectively (Figure 8a). The drug release was tuned by adjusting the exposition time to the NIR light (Figure 8b). The presence of AuNRs and graphene increased the local temperature and reduced the exposition of the cells to be damaged by the IR source. An illustration of the NIR source arrangement and the samples are shown in Figure 8c.

In addition to their applicability in drug delivery, the utilization of hybrid TSHs in catalysis, antibacterial coatings, soft robotics, and sensors is also the subject of intense research. Risse and coworkers^[108] studied the kinetics of the reduction of 4-nitrophenol to 4-aminophenol catalyzed by nanoreactors containing a core of polystyrene (PS) and a shell of PNIPAAm-Ag nanoparticles (Ag@PS-PNIPAAm). Results revealed a dependence of the conversion with the temperature applied, even though they did not follow the Arrhenius law. Then, the Ag nanoparticles (AgNPs) were adsorbed on the shell of the TSH nanoreactor and the increase or decrease of the LCST temperature of the hydrogel was used to regulate the conversion.

More examples of PNIPAAm combinations with inorganic materials will be approached in the following sections according to their application main fields.

4. Biomedical Emerging Applications of Poly (N-isopropylacrylamide) and Derivatives

In the biomedical field, PNIPAAm is the most popular temperature-responsive polymer investigated.^[10] This

stimuli-responsive hydrogel and its copolymers have been proved to be biocompatible^[2] and have enhanced adhesion towards several substrates (glass, metal, and plastics).^[109,110] Thus, both properties are attractive to explore new horizons for their uses in biomedicine.

In the following sections, the most important systems investigated until now, by combining TSH and other compounds, will be detailed described.

4.1. Uses of Poly(N-isopropylacrylamide) Thermosensitive Hydrogels and Derivatives in Biomedical Field

4.1.1. Thermosensitive Hydrogels in Drug Delivery Systems (DDS) Applications

Various hydrogel-based dosage forms based on TSHs have been developed to better target and control the current systems.^[111]

In the ophthalmic field, the low bioavailability of eye drops due to rapid clearance action induced by tear dilution and the lacrimal drainage system represents a limitation. Luo et al.^[112] demonstrated effective topical treatment of dry eye disease (DED) through a mucoadhesive drug delivery system based on TSHs.^[112] Specifically, the design of the material involved a drug carrier that consisted of a chemically ternary material system made of gelatin (GN), which served as an enzyme-mediated degradable matrix; a thermoresponsive regulator, which was represented by the PNIPAAm; and a mucus-binding component, which was lectin *Helix pomatia* agglutinin. The resultant biodegradable, mucoadhesive, and thermoresponsive hydrogel provided a sustained release of epigallocatechin gallate molecules and elevated the drug bioavailability above therapeutic levels

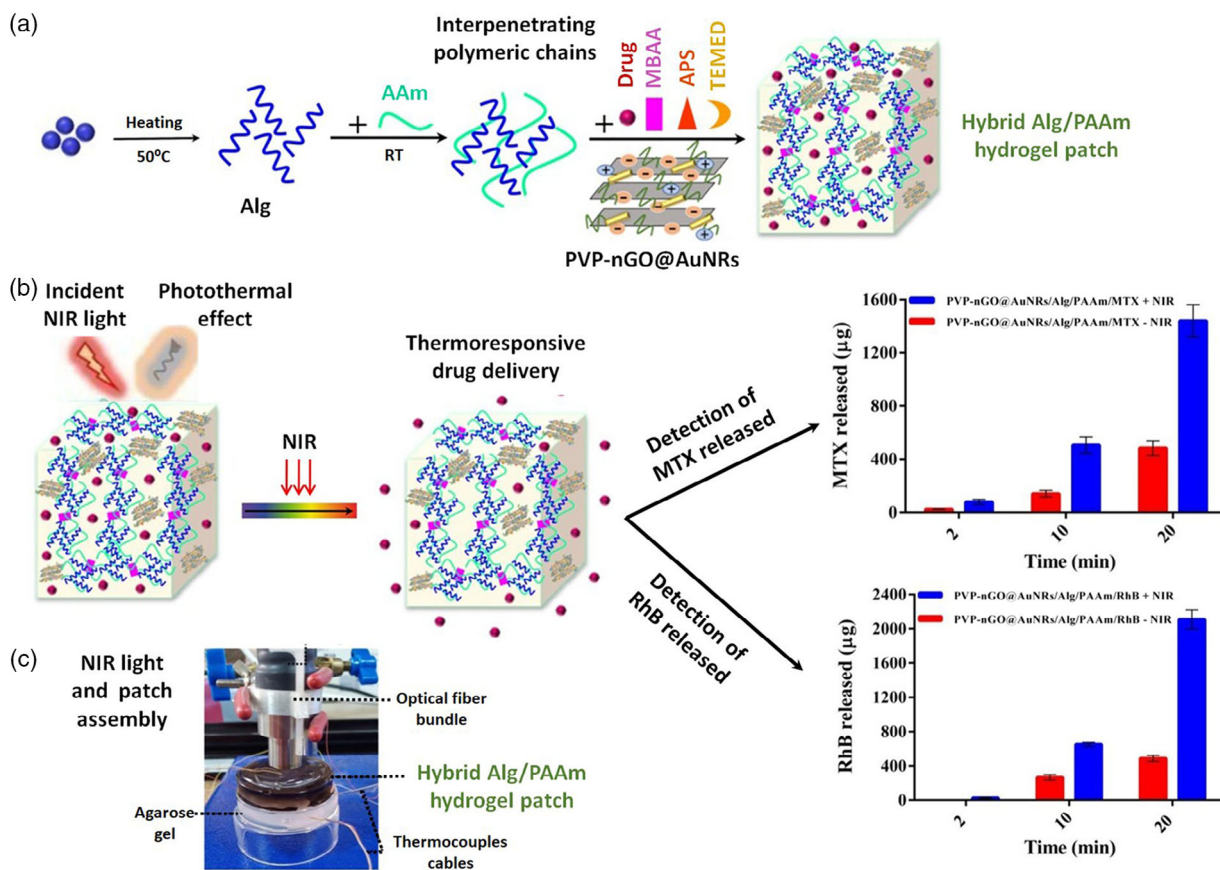


Figure 8. a) Scheme of synthesis and preparation of TSH patch composed of natural (ALG) and synthetic (PAAm) hydrogels, intercalated with sheets of poly(vinylpyrrolidone) functionalized with graphene and AuNPs, to potentiate the photothermal effect under NIR light. b) Example of drug- and dye delivery under NIR activation (images on left) and amount released with time (plots on right). c) Photograph of NIR optical fiber above the hybrid hydrogel and system to measure the temperature of the hydrogel, employed in this study. the hydrogel, employed in this study. Reproduced with permission.^[107] Copyright 2020, Elsevier.

for a period over 14 days.^[112] In the same field, Zhu et al.^[113] developed an in situ gelling formulation of ketoconazole based on PNIPAAm/hyaluronic acid. In this study, high drug content was achieved (91–96%) at slightly acid and neutral pHs (i.e., pH 6.0–7.5), the gelation temperature being of 33 °C.^[113]

Current treatments for oral mucosa-related ulcers use drugs to relieve pain and promote healing, but rarely consider drug resistance to bacterial infection in the microenvironment of the oral cavity or the prevention of bleeding from gingival mucosa ulcers. Recently, an injectable, thermogelling chitosan-based system was produced to address these concerns.^[51] An aqueous solution of chitosan-based conjugates, in particular, chitosan-g-PNIPAAm-g-polyacrylamide (PAAm) graft copolymer could reversibly form semi-solid gels at physiological temperatures and inhibit both Gram-positive and Gram-negative bacteria. The systems with the highest chitosan and PNIPAAm contents were found to promote the proliferation of gingival fibroblasts in vitro and exhibited improved blood clotting in an in vivo rat study (Figure 9a).^[51] To fabricate a smart thermo-pH stimuli responsive drug delivery system for cancer therapy, TSHs based on PNIPAAm-doxorubicin (PNIPAAm-DOX) hydrogel were synthesized and loaded into pH-responsive poly ethylene glycol-2,4,6-trimethoxy

benzylidene pentaerythritol carbonate (PEG-PTMBPEC) polymersomes.^[69] The TSHs formulation revealed a small dimension (170 ± 11.2 nm) and encapsulation efficiency of about 31%. In vivo release evaluation assays demonstrated that the DOX release was pH-dependent (i.e., faster at pH lower than the physiological one) and, that the drug release was significantly decreased at 37 °C due to the gelation of PNIPAAm-DOX conjugate in the interior compartment of the pH-responsive polymersomes.^[69] The pharmacokinetic profile evidenced that the prepared smart hydrosomal formulation significantly increased the blood half-life time of the drug and modified the biodistribution.^[69] Treatment with the polymersomal formulation did not cause any systematic toxicity in terms of pathological alteration of vital organs, survival rate, and body weight loss system. Moreover, the tumor growth rate was significantly inhibited in mice receiving a single dose via either intravenous or intratumoral injection in comparison with the free DOX-treatment group.^[69]

Lu et al.^[114] prepared nanoparticles of about 70–90 nm of poly(flourene-co-vinylene) (PFV), a conjugated polymer, charged with DOX drug and covered by a layer of PNIPAAm molecules, by nanoprecipitation of the mixed organic solution in water. They called the resulting nanocarriers as PNIPAAm-DOX-conjugated

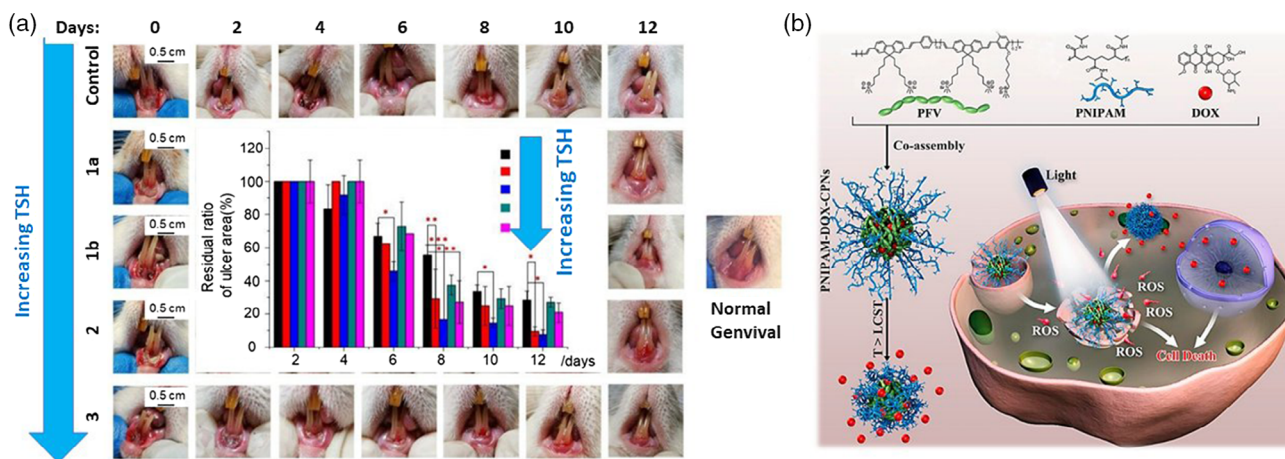


Figure 9. a) Healing of gingival ulcers in Sprague Dawley rats after treatment with chitosan-based thermogels, with increasing time. In the graph inserted, a high reduction of ulcer relative residual area can be seen with time and with increasing TSH content. Data are presented as means of standard deviation and significance was analyzed using two-way ANOVA and Bonferroni post-tests ($n = 3$, $*p < 0.05$, $**p < 0.01$, $***p < 0.001$ in comparison with the Control group). Reproduced with permission.^[51] Copyright 2020, Royal Society of Chemistry. b) Schematic illustration of the formation of thermal-responsive nanoparticle (PNIPAAm-DOX-CPNs), drug release, and chemo-/PDT synergistic therapeutic mechanism. Reproduced with permission.^[114] Copyright 2019, American Chemical Society.

polymer nanoparticles (CPNs). This new system proved to have a significant effect on the DOX release, potentiated by the collapse of the PNIPAAm chains and the expulsion of the hydrophilic drug (Figure 9b). In vitro drug release experiments demonstrated that, at pH 5.5 (slightly acid) and 37 °C (above PNIPAAm LCST), more than 70% of DOX was released because the NPs agglomerated, induced by the PNIPAAm contraction and the protonated drug could be expelled due its higher hydrophilicity in such media. They also observed a great stability of the PFV-DOX NPs in PBS, attributed to the presence of PNIPAAm. The conjugated polymer PFV acted as a photosensitizer to produce high reactive oxygen species (ROS) under white light irradiation. The combination of the polymer with the TSH proved to be a promising nanocarrier for effective chemo-/photodynamic therapy (PDT) in future cancer treatments.^[114] More investigations would be desirable to evaluate the toxicity of the whole system in vivo.

4.1.2. Thermosensitive Hydrogels in Wound Healing Applications

In the field of wound healing, many researchers focused their attention on the design and production of new materials. Very recently, Banerjee et al.^[115] reported a new wound-healable material based on AgNPs embedded thermoresponsive multilayered micellar inter-polyelectrolyte complex (IPEC) hydrogel, prepared via reversible addition fragmentation chain-transfer (RAFT) polymerization. The preparation of the IPEC complex was carried out via the interlocking of two ionic AB-type block copolymers: an inner thiolated cationic poly(2-hydroxyethyl methacrylate-block-poly(2-(methacryloyloxy)ethyltrimethyl ammonium chloride) (PHEMA-b-PMTAC) stabilized with AgNPs; an outer anionic thermoresponsive poly(*N*-isopropylacrylamide-block-sodium 4-vinylbenzenesulfonate) (PNIPAAm-b-PSS) moiety with a flower-like morphology.^[115] In vitro and in vivo studies confirmed the suitability of this material for wound-healing

application, showing that tissue regeneration was more effective when AgNPs were incorporated into TSHs.^[115]

In a recent study, Han et al.^[116] reported poly(*N*-isopropyl acrylamide)/keratin double network (PNIPAAm/keratin DN) gels fabricated through a covalent and ionic double cross-linking strategy. Such TSHs exhibited multiple-responsiveness (temperature, pH, and ROS), excellent antibacterial activity and a faster wound healing rate. Indeed, in vivo wound healing results evidenced more new born blood vessels and higher collagen volume fraction than commercial wound dressing Tegaderm (Figure 10a).^[116] The wound healing rate for 14 days was measured as well, demonstrating that the hydrogel-treated group showed significant visual improvement compared with the untreated group and the 3 M Tegaderm group.^[116]

One of the most powerful and versatile methods to fabricate polymer devices is the 3D printing technology. Interestingly, Nizioł et al.^[117] employed this technology to prepare a hydrogel ink, composed of synthetic and natural precursors, for wound dressings with an incorporated antimicrobial agent. The printable ink containing PNIPAAm precursors, sodium ALG, MC, which was mixed with octenidine dihydrochloride and 2-phenoxyethanol (Octenisept, OCT) antiseptic commercial product, was evaluated, showing outstanding printability (Figure 10b). This study provided the protocol of ink's use for the 3D printing of hydrogel scaffolds with good antimicrobial activity for wound healing applications (external use).

Blacklow et al.^[118] developed a novel design of mechanotherapeutic device for wound dressing, which activated and accelerated the healing. In this work, a new paradigm for wound management was presented, which was inspired by embryonic wound contraction and took recent advances in hydrogels and adhesives.^[118] This work led to active adhesive dressings (AAD), which were able to form strong adhesion to skin and generate sufficient contractile strains in response to skin exposure

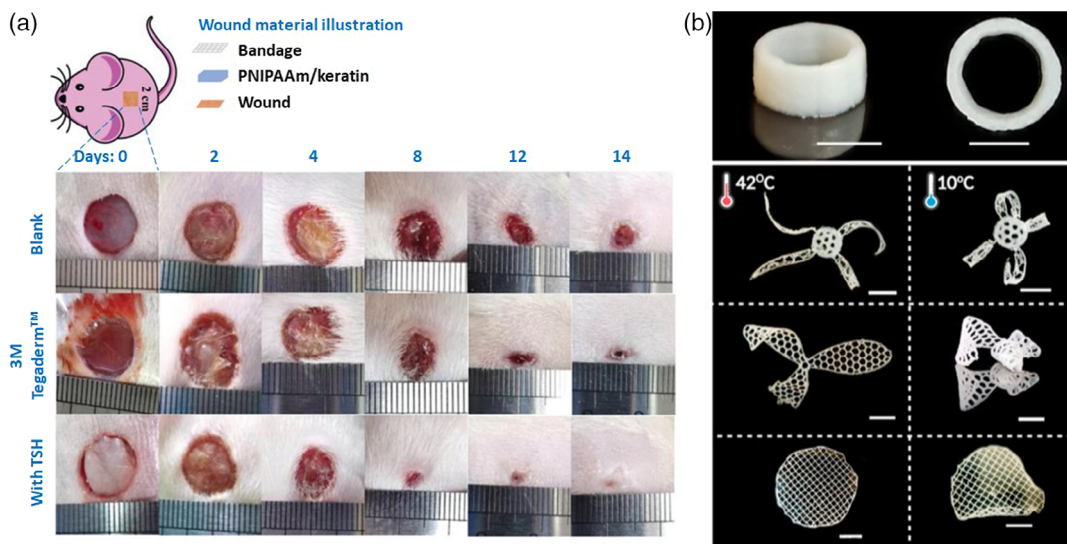


Figure 10. a) Schematic illustration of the wound and treatment schedule in rats and macroscopic observation of rat wounds at different time intervals treated with the blank, 3 M Tegaderm dressing, and PNIPAAm/keratin DN gels; Reproduced with permission.^[116] Copyright 2021, Royal Society of Chemistry. b) Four different 3D-printed scaffold models fabricated with a hydrogel ink composed of PNIPAAm/ALG:MC (1:1) and charged with OCT antimicrobial agent. The authors demonstrated that OCT release is potentiated at temperatures of 37°C thanks to the presence of the TSH. Scale bar corresponds to 1 cm. Reproduced under the terms of a Creative Commons Attribution CC-BY license.^[117] Copyright 2021, The Authors, published by MDPI.

temperature to enhance healing. The newly reported ADD consisted of a hybrid PNIPAAm-ALG network that contracts wounds at the physiological temperature, accelerating and supporting skin wound healing as demonstrated by *in vitro* and *in vivo* studies.^[118]

All the above-mentioned studies give us one idea of how natural and synthetic TSHs would influence the next generation of dressings, antiseptic films, among other biomedical materials, development.

4.1.3. Thermosensitive Hydrogels in Bioseparation and Bioanalysis Studies

TSHs-based chromatography technique system was also investigated to purify and separate a variety of proteins and cells.^[119–121] Temperature-responsive HPLC columns and temperature-responsive solid-phase extraction (TR-SPE) columns were found to work as effective separation tools for monoclonal antibodies, nucleic acid drugs, and cells. In another work,^[122] a new device for bioanalysis was manufactured using a poly(NIPAAm-co-BMA-co-DMAPAAm) (where BMA is *n*-butyl methacrylate and DMAPAAm is *N,N*-dimethylaminopropyl acrylamide) hydrogel modified TR-SPE system, in which silica beads with average diameters ranging from 100 to 150 μm were employed for optimizing the column towards the size of blood cells. Temperature-dependent cell elution behavior was observed in the separation of HL-60 and Jurkat cells (leukemia cells). Cell retention and elution behaviors were changed by varying the content of the cationic group in the copolymers and by modulating the temperature. As reported in **Figure 11a**, cells were retained in columns containing beads with cationic properties at 37°C, whereas beads without cationic properties did not retain the cells. Cells were

later eluted at 4°C because of reduced hydrophobic interactions, while the retention at 37°C occurred through electrostatic interactions. Nagase et al.^[123] developed a block copolymer brush with bottom poly(2-hydroxyethyl methacrylate [HEMA]-*co*-propargyl acrylate) and top poly(*N*-isopropylacrylamide-*co*-HEMA) (where HEMA is hydroxyethylmethacrylate) segments. The complex system was synthesized using a two-step procedure: atom transfer radical polymerization followed by the conjugation of cell affinity peptides to the bottom segment of the copolymer brush through a click reaction. Using a cyclic RGD peptide (cRGD) as a cell-affinity peptide, enhancement of cell adhesion with rapid adhesion on the copolymer brush was observed at 37°C, whereas the copolymer brush without cRGD did not exhibit cell adhesion. Temperature-modulated cell adhesion and detachment were performed with a relatively long upper segment because the affinity between peptides and cells was modulated by the swelling and shrinking of the upper thermoresponsive segment.^[123]

Controlled radical polymerization by reversible addition-fragmentation chain transfer (RAFT) was employed to fabricate double-layered, non-cytotoxic surfaces beneficial for the cell sheet attachment/detachment process.^[124] Radiation-induced grafting of poly(acrylamide) (PAAm) from PS cell-culture Petri dishes and subsequent chain extension of the grafts by poly(*N*-isopropylacrylamide) (PNIPAAm) was achieved by pre-irradiating PS with an electron beam. The RAFT polymerization permitted to control the thicknesses of both blocks on nanoscale, which is crucial for cell sheet engineering. Water contact angle measurements demonstrated that dishes modified by PAAm-block-PNIPAAm brushes showed significant temperature-dependent interfacial properties in aqueous media.^[124]

Recently, the effects of terminal cationization and length of grafted PNIPAAm chains on temperature-dependent cell

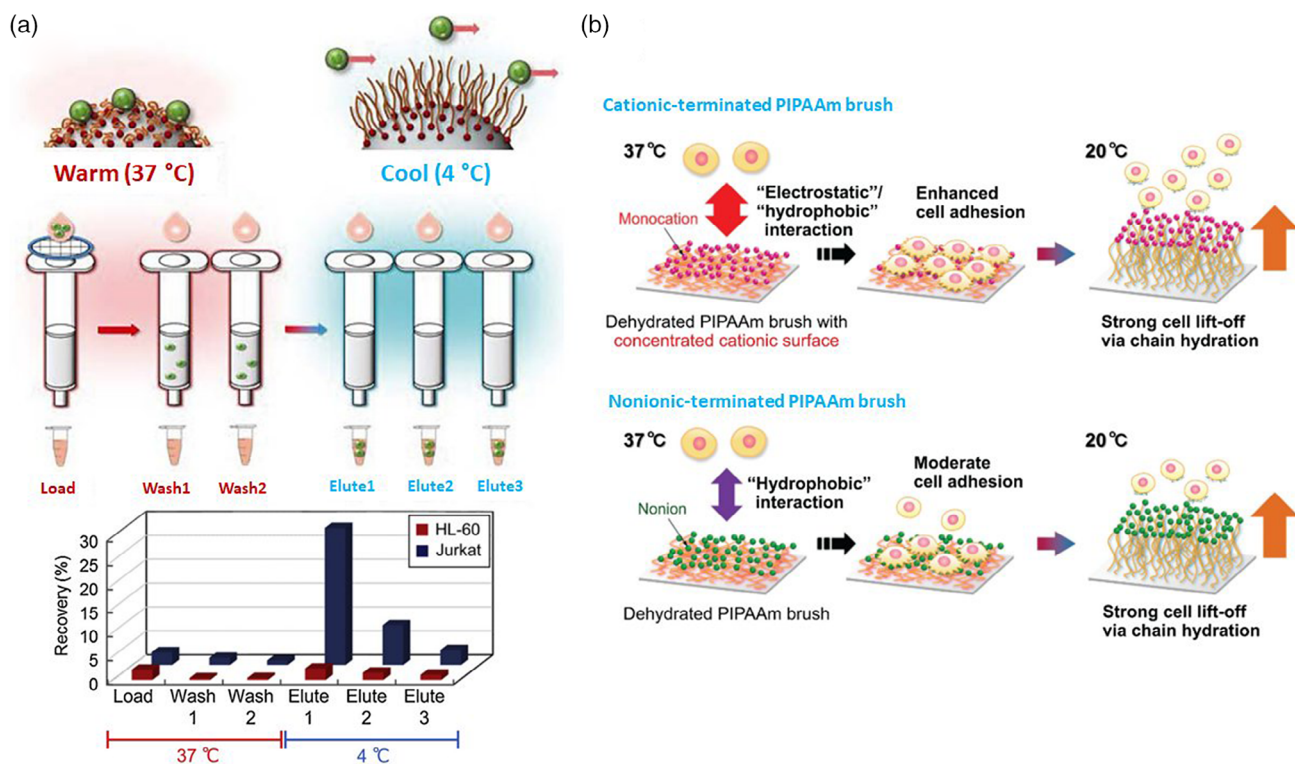


Figure 11. a) Temperature-modulated cell separation using P(NIPAAm-co-BMA-co-DMAAm) hydrogel-modified TR-SPE column. Concept of interaction between polymer-modified surface and cells, protocol of cell separation using TR-SPE column, and corresponding elution profiles of HL-60 and Jurkat cells. Reproduced with permission.^[122] Copyright 2021, Springer Nature. b) PNIPAAm brush-modified substrates (PIPAAm brush, as called in the reference) with a terminal cationic group prepared via RAFT polymerization. Cationized PNIPAAm surfaces showed markedly high cell adhesion compared with nonionized ones. Reproduced under the terms of a Creative Commons Attribution CC-BY license.^[125] Copyright 2021, The Authors, published by National Institute for Materials Science in partnership with Taylor & Francis Group.

adhesion–death were investigated.^[125] PNIPAAm brushes with three chain lengths were grafted on glass coverslips via RAFT polymerization surface initiated and terminal substitution with either monocationic trimethylammonium or nonionic isopropyl moieties was performed (Figure 11b). Interestingly, cationized PNIPAAm surfaces showed markedly high cell adhesion compared with nonionized ones. It was attributed to the monocations concentrated at the periphery of the dehydrated PNIPAAm brushes. Furthermore, longer PNIPAAm chains reduced cell adhesion because of the increased surface hydrophilicity but accelerated cell detachment from the thermoresponsive surfaces.^[125]

4.2. Advanced Diagnosis Approaches by Combining Thermosensitive Hydrogels with Other Materials

The development of multifunctional biomedical devices is one of the pioneering emerging fields with increase investigations in TSHs. However, the plastics used as a substrate to prepare the biomedical platforms or the hydrogels are non-responsive materials, hindering the detection of implants or prosthesis once inserted in the body. Then, one successful strategy is to use plasmonic particles to be able to take the advantage of semi-invasive spectroscopy diagnosis tools.

For instance, Quidant and coworkers^[126,127] demonstrated the plasmon-enabled inactivation of bacteria after stimulation of PP yarn surface, functionalized with Au@citrate-stabilized NPs, with near-infrared spectroscopy (NIR). However, the big disadvantage of using NIR is the extremely high temperature the laser can reach, causing also the death of good cells. Nowadays, Raman spectroscopy seems to be more promising than NIR, with the advantage of a lack of negative effect on live cells or in the degradation of biomedical plastics.

Recent advances in the employment of plasmonic NPs serve as the foundations for rapid progress in unusual spectroscopy applications of surface-enhanced Raman scattering (SERS) in the medical field. The most renowned and driving force researcher behind the development of this type of bio-imaging and bio-marker detection by using plasmonic effect and Raman vibrational spectroscopy is Prof. Liz-Marzán.^[128] Álvarez-Puebla and Liz-Marzán^[129] were the first to describe the preparation of AuNPs with PNIPAAm as shell (Au@pNIPAM) for SERS applications. Moreover, they evaluated the influence of LCST in the Raman-enhanced spectroscopy signal. More recently, Bodelón et al.^[130] were able to detect three tumor-associated protein biomarkers (in vitro) using Au@pNIPAM microgels and an excitation laser of 633 nm. Both works proved the potential application of such particles in the biomedical field.

In SERS technology, there are several factors that can affect the target detection, such as: 1) metal NP core (nature, morphology, etc.); 2) NP shell nature; 3) nature of molecules used to stabilize the NP shell (sodium citrate ascorbic acid, surfactant mixtures, etc.); 4) nature of molecules used as fingerprint labels (called SERS nanotags or RaRs, Raman reporters); 5) the thickness of the coating used to encapsulate the metal-based NPs; among others.^[131] Fortunately, most of them are well controlled and the signal can be enhanced by choosing the correct Raman excitation source and probes. For example, Gambhir and coworkers^[132] developed a small animal Raman instrument for rapid and wide-area spectroscopic imaging by using SERS NPs injection in mice, as well as a complete Raman system for SERS in vivo imaging detection of inflammatory processes in human by endoscopy intervention.

For instance, the full conversion of PP meshes, used in hernia repair, modified with PNIPAAm hydrogel and Au NPs (PP-g-PNIPAAm@AuNPs), to a spectroscopic detectable material has recently been reported by our group.^[133] With plasma activation and covalently bonded AuNPs we were able to distinguish the presence of 4-mercaptiothiazole (4-MB), the RaR molecule, inside the layer of PNIPAAm hydrogel and above the PP yarns used as substrates, either using 532 or 785 nm irradiation sources (Figure 12). The complex architecture of the mesh material (textile fabrication, different densities, and pore sizes) did not affect the sensitivity of the analysis. Nevertheless, further investigations with SERS in vivo imaging would be desirable for the

semi-invasive detection of the PP-g-PNIPAAm@AuNPs new implants to certify that body fluids or organs will not interfere with the spectrum recording.

4.3. Biomedical Sensors

The thermoresponsive properties of PNIPAAm have been used to engineer different types of sensors, such as piezoelectric,^[134–139] irradiation,^[140–142] optical,^[143] luminescent,^[144] electrochemical,^[145–150] humidity,^[151] and plasmonic.^[152–154] This section reviews how the response capacity of PNIPAAm against external stimuli has been used to detect different analytes and chemical parameters using different sensing elements and signals.

Although piezoresistive sensors have been successfully prepared by regulating the rate of swelling and de-swelling of PNIPAAm hydrogels through their porosity,^[134,135] faster and much more versatile responses have been achieved by interpenetrating that hydrogel with other components. For example, thermoresponsive nanostructured PNIPAAm hydrogel was interpenetrated by in situ polymerization with light absorbing and conducting polypyrrole (PPy) to achieve an ultra-stretchable self-sensing remotely triggered actuator.^[136] In such a self-monitoring device, PPy acted as a photothermal transducer and electrical conductor, while de-swelling of the PNIPAAm hydrogel produced a volume shrinkage that facilitated the percolation of the PPy network (Figure 13a). This allowed the creation of

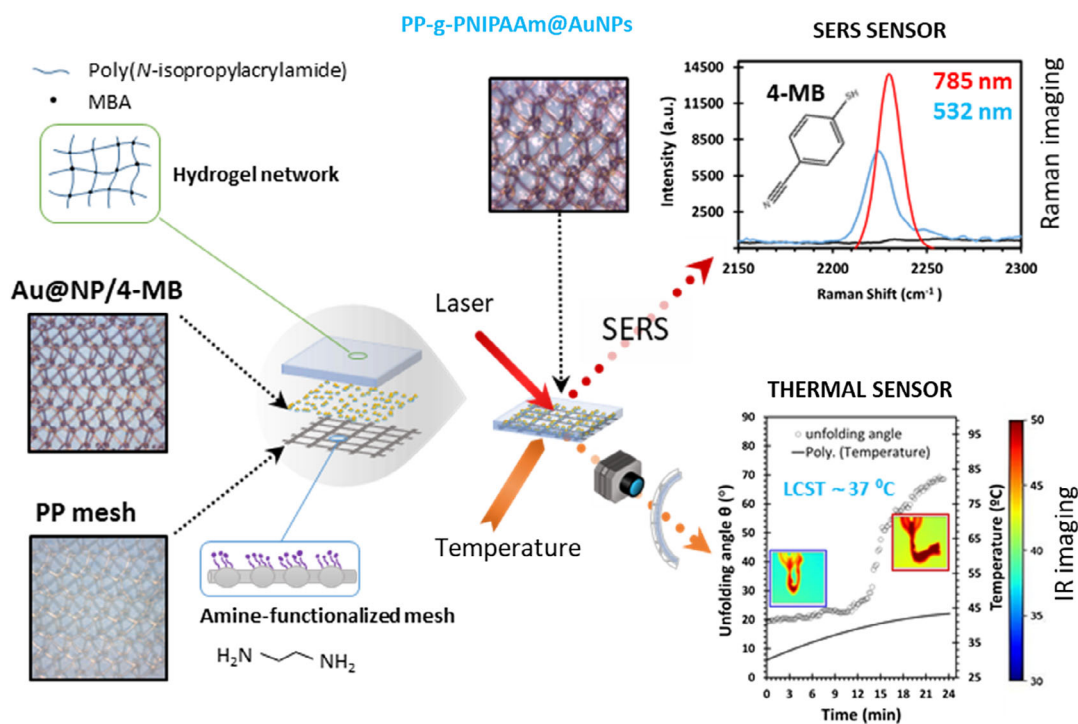


Figure 12. Illustration of the conversion of PP mesh prosthesis to a SERS responsive material after functionalization with AuNPs/4-MB and PNIPAAm-co-MBA hydrogel (on left and on middle images). On right side images, exemplified on top represent the Raman spectra with different source excitations (532 and 785 nm) to detect the most important absorption band of RaR molecule (4-MB), trapped in gold NPs and in the interface between PP substrate and TSH coating. Reproduced with permission.^[133] Copyright 2022, American Chemical Society. On the bottom right, the plot represents the effect of expansion/contraction of PNIPAAm chains, under temperature variations and increasing time, founding an LCST transition of 37 °C, 5 °C higher than the same system without AuNPs/4-MB). Adapted with permission.^[89] Copyright 2020, Wiley-VCH.

untethered soft robots with unprecedented sensory capacities (Figure 13b). A similar strategy was followed using conducting PANi.^[137] In this case, the PNIPAAm/PAni double network was used to manufacture a system to disconnect circuits when, upon reaching a high temperature, a volume change occurs in the interpenetrated hydrogel. Amazingly, no interpenetrated PNIPAAm was reported with poly(3,4-ethylenedioxythiophene) (PEDOT),^[155] which is not only the most stable conducting polymer being explored but also the most used in biomedical applications due to its high biocompatibility, conductivity, and stretchability.^[156–158] In another approach, PNIPAAm was combined with ionic hydrogels, for example, the one prepared using polyvinyl alcohol (PVA), sodium tetraborate decahydrate and sodium polyacrylate,^[138] or metallic nanoparticles,^[139] for example, allyl mercaptan functionalized AuNPs, to create flexible and stretchable systems able to respond against touch and temperature stimuli simultaneously. However, the results achieved using such a strategy are similar to those that could be obtained by using CPs, which are also able to provide flexibility, stretchability, and a linear variation of the conductivity against pressure.^[159]

A thermoresponsive hydrogel to detect microwaves irradiation was prepared using PNIPAAm cross-linked by a polydiacetylene-containing layered composite.^[140] The heating of water in the hydrogel, which increased with the microwave irradiation time,

resulted in a gradual color change (Figure 13c). In contrast, Robby et al.^[141] used NIR light to detect the electronic state of carbon quantum dots using a sensor made by loading polydopamine-functionalized fluorescent carbon dots into PNIPAAm hydrogel. Similar concepts, which are based on PNIPAAm conformational changes upon irradiation, were used to detect proteins with a hydrogel in which PANi nanofibers modified with graphene oxide acted as physical cross-linker of the PNIPAAm chains.^[142] Despite these advances, the use as a sensor of the thermal response induced in the PNIPAAm by irradiation is still very incipient and, therefore, many more studies are needed to improve the relationship between said response and the type of radiation, depending on the desired application.

In the field of optical sensors, ultra-sensitive detection of a steroid hormone (progesterone) was achieved by functionalizing a layer of PNIPAAm microgel with specific antibodies, which was subsequently sandwiched between semi-transparent gold layers supported on glass (Figure 14a).^[143] The binding of the antibody molecules induced the collapse of the microgel producing the optical response of the device, which exhibited visual color and multi-peak reflectance spectra. The limit of detection of this sensor was as low as 0.28 ng mL⁻¹ at room temperature. Besides, promising luminescent sensors for

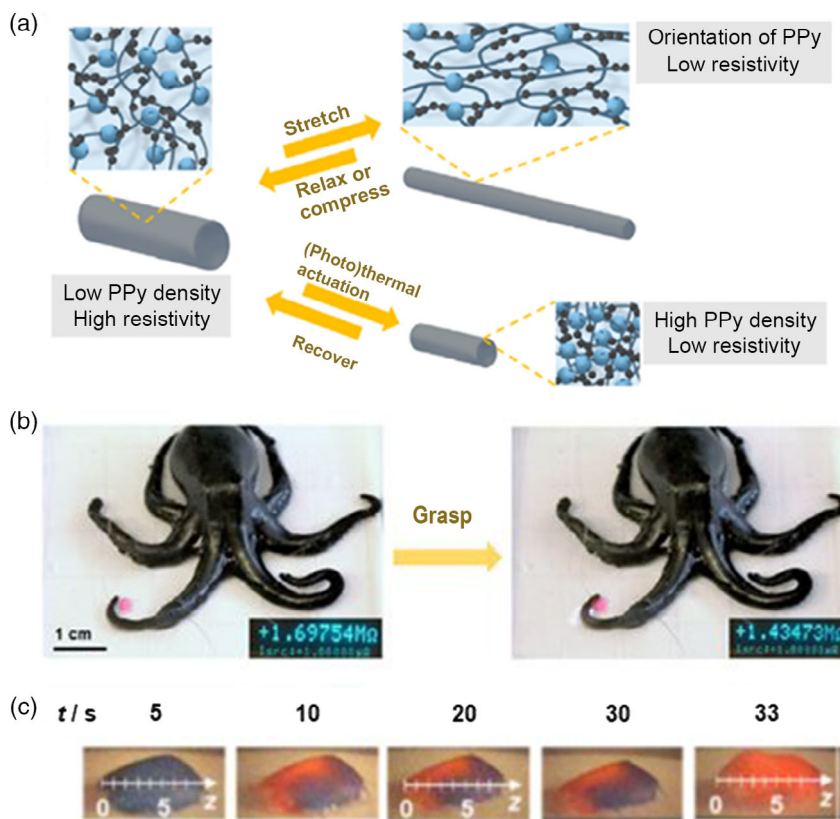


Figure 13. For the PNIPAAm/PPy piezoresistive hydrogel sensor: a) Resistivity changes with stretching, compression, and photothermal actuation due to changes in alignment and apparent density of the conducting PPy network. Reproduced with permission.^[136] Copyright 2021, Elsevier. b) Self-sensing grasping motion by NIR manipulated local stimulation. Reproduced with permission.^[136] Copyright 2021, Elsevier. c) For the PNIPAAm/polydiacetylene hydrogel sensor to detector microwave irradiation: Photographs showing the change of color with increasing irradiation time (5, 10, 20, 30, and 33 s). Reproduced with permission.^[140] Copyright 2020, American Chemical Society.

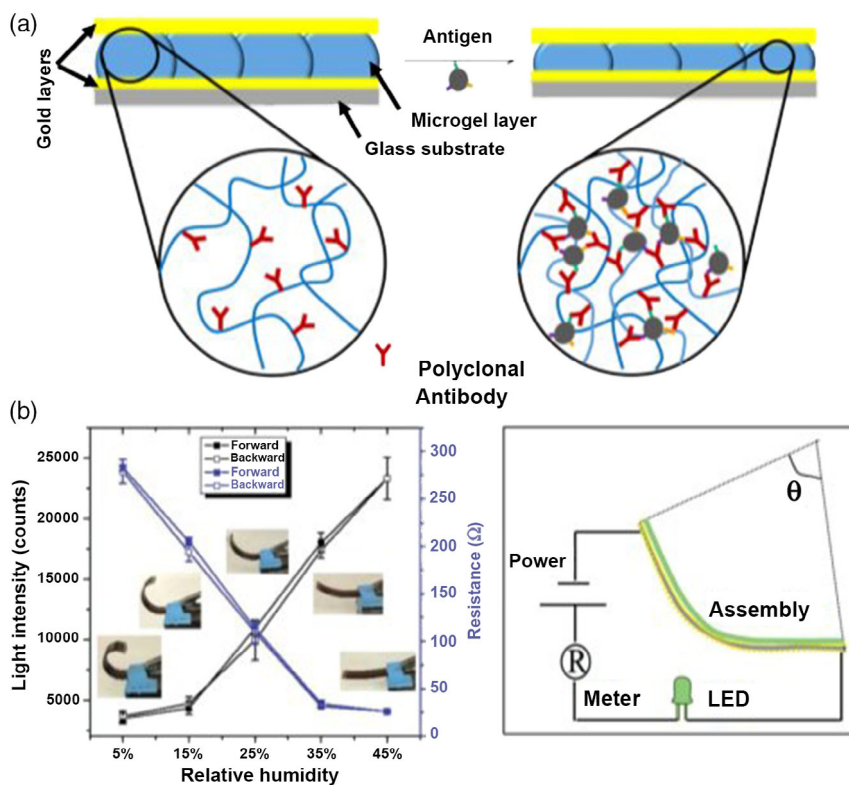


Figure 14. a) Sketch of the optical sensor constructed with PNIPAAm microgel and semi-transparent gold layers for the detection of progesterone. Reproduced with permission.^[143] Copyright 2016, Springer Nature. b) For the PNIPAAm-based humidity sensor: Light intensity (left axis), resistance (right axis), and degree of bending (photographs) against the relative humidity (left side). The right side depicts the light-emitting diode (LED)-containing an electric circuit used to measure the light intensity and the resistance as a function of the degree of bending (i.e., relative humidity). Reproduced with permission.^[151] Copyright 2016, Wiley-VCH.

the detection of cationic surfactants were prepared using quinoline-labeled thermosensitive PNIPAAm, which exhibited pronounced temperature-controlled luminescence response upon association with cationic surfactants, changing from green to blue.^[144]

Thermal-switchable systems for electrochemical detection have been also reported using a combination of PNIPAAm (nano)hydrogels and electrochemically responsive materials.^[103,145–150] The choice of the latter was decided primarily on the basis of their advantages in terms of sensitivity, selectivity, and stability. Among the utilized electroactive materials, ruthenium nanoparticles,^[147] palladium nanoparticles dispersed on graphene sheets,^[150] silica nanoparticles functionalized with glucose oxidase,^[149] PANi with copper ions,^[103] poly(3,4-ethylenedioxythiophene),^[146] CNT-cellulose nanocrystals,^[148] and CNT-graphene quantum dots,^[145] deserve special mention due to their successful electrochemical response. The combination of those materials with PNIPAAm enabled the temperature-reversible “on/off” electrochemical detection of antibiotic sulfamethazine,^[147] 4-nitrophenol,^[150] glucose,^[103] herbicide acifluorfen,^[103] antineoplastic drug 5-fluorouracil,^[146] lactate,^[148] and paracetamol,^[145] respectively. Within this context, the incorporation of PNIPAAm provides great advantages with respect to the use of electroresponsive materials alone, since it allows including of a selective effect depending on the temperature that is not easy to achieve with other materials.

In contrast, humidity sensors have been also manufactured using PNIPAAm-based microgels. More specifically, bilayered stretchable and bendable sensors composed of polydiallyldimethylammonium chloride deposited on a single layer of microgel, which was attached to a semi-flexible gold support, were reported to measure the humidity of the environment.^[151] Thus, the degree of bending of such a bilayered system was found to depend on the humidity, decreasing with increasing humidity. This phenomenon was coupled to a change in the material conductivity, which was proved by connecting this system to a circuit with a light-emitting diode (LED) (Figure 14b). Inspection of the variation of the sensor bending, the resistivity, and the LED light intensity as a function of the humidity is included in Figure 14b. As can be seen, the light intensity increased, due to the decreased electrical resistance, with the humidity. Despite this being an outstanding application, no sensor has been yet interconnecting the responses of PNIPAAm and their derivatives towards both the humidity and the temperature.

Finally, plasmonic technology was also used to develop sensors with enhanced sensitivity. For instance, Lee et al.^[152] intercalated a thermoresponsive PNIPAAm layer of nanometric thickness between gold substrate and AuNPs. Quantitative changes in surface plasmon resonance signals were observed when the temperature increased from 20 to 32 °C, which caused a reduction from 30 to 14 nm in the thickness of the PNIPAAm layer. This caused an improvement in the refractive sensing with

respect to the control, which was around 20%. Similar principles were recently applied by Causa and coworkers^[153] and by Whitten and coworkers^[154] for developing melamine and light-sensitive gas sensors, respectively, using functionalized PNIPAAm and plasmonic AuNPs.

5. Thermo-responsive Hydrogels for Water Treatment

Nearly 98% of the water resources on earth are stored as either seawater or brackish water. Desalination comprises a nonconventional water resource practice that is able for filling the gap in the water balance supply. The most widely used processes in desalination plants are reverse osmosis (RO), forward osmosis (FO), and thermal separations, such as membrane distillation (MD).^[160] All such chemical engineering processes require the consumption of semipermeable membranes fabricated with polymers, usually multilayered and arranged with ceramic and hybrid materials. However, the membrane's and filter's costs, foiling problems, and the large amount of residue generated after the water purification (for 1 L of pure water, ≈ 2 kg of waste), added to the fact that traditional desalination consumes a large amount of energy and produces huge greenhouse gas emissions, represent a persistent drawback.

In this sense, hydrogels are emerging as powerful alternatives to the classical materials usually employed in water purification. TSHs applied for solar-driven water evaporation and desalination are experiencing increasing interest since 2017. The most prominent works belonging to North America^[161–163] and China.^[164–166]

5.1. Thermosensitive Hydrogel for Solar Desalination

In desalination technologies, PNIPAAm has attracted attention as an innovative and alternative material suitable to achieve a reduction of energy consumption. For instance, Zhao et al.^[16] described a FO process based on the use of poly (sodium styrene-4-sulfonate-co-N-isopropylacrylamide) membranes, which could be regenerated at 50 °C through membrane distillation, having thermal consumption of around 29 kWh m⁻³ and electrical consumption less than 4 kWh m⁻³, and with a mass flux rate of 4 kg m⁻² h⁻¹ (KMH) of seawater cleaned. Such reference data, which were used by authors to conclude that the TSH behavior facilitates draw solution regeneration compared to other systems, also provided valuable insights into the weak points of this technology and guidelines for its further development.

Pioneer research in solar water desalination was developed by Yu and coworkers, who combined hydrogels and conducting polymers.^[167,168] The research was based on a mechanism that involved the adjustment of different states of water in a polymer network with a porous hydrophilic structure, thereby reducing the heat required for vaporization. The utilization of a hydrogel made of PVA/chitosan copolymer and PPy as stimulus-responsive additive, allowed to design a highly efficient prototype, able to evaporate 2.5 KMH of brackish water with radiation energy equivalent to 1 kW m⁻² (or 1 sun) (Figure 15a–c).^[161] Moreover, in the outdoor solar desalination the water evaporation

rate, which is independent of salinity, was maintained up to 50 h after continuous exposure of the hierarchically nanostructured gel (HNG) to natural irradiation (i.e., natural sun light). Another example, which was based on PNIPAAm hydrogel doped with PPy-chlorine, with adjustable hydrophilicity, was reported by the same authors.^[168] They found that the evaporation rate exceeded 3.0 KMH under 1 sun illumination, while the light-to-evaporation conversion efficiency approached 100%. As a result, the daily freshwater production was very high (18–23 L m⁻² day⁻¹), proving that technologies based on TSHs are powerful tools to reduce the consumption of urban water in city hall facilities.

Other pioneering researches that successfully combined TSHs with conductive materials (essentially graphene) to obtain clean water, were reported by Prof. Liangti Qu and coworkers.^[164,165,169] Those authors devised a system to purify water (output) from shower, clothes, and dish washers (input water) for its subsequent application not only in similar or other domestic uses but also in industry (Figure 15d). It was demonstrated that many types of wastewater, even raw pharmaceutical wastewater, can be purified by solar evaporation (Figure 15e). The reported prototype consisted of a highly vertically ordered pillar array structure of graphene framework (abbreviated as HOPGF) (Figure 15f), which could be installed on the transparent roof of buildings to receive natural light. This is one example of visionary research whose prototypes may end up reaching the market and becomes one more tool against climate change in areas with water stress: recovery of urban water (from domestic waste, rain reservoirs, etc.) and purification for self-consumption (Figure 15g).

Overall, reported results suggest that methods for desalinating seawater using solar energy and conducting polymer hydrogels (CPHs) or graphene hydrogels (GHs) could be viable. Among the potential advantages of such technologies, the reduction of energy costs as well as their possible application in offshore and remote areas, are particularly promising and deserve special consideration.

For mass production, there are other promising and consolidated technologies able to generate freshwater from low-salinity water,^[170] for example, electrodialysis (ED), capacitive deionization (CDI), ion concentration polarization, desalination batteries, and microbial desalination cells.^[171] Among such technologies, CDI has attracted more attention, in recent years, because of its reduced energy consumption, environmental friendliness, and no secondary pollution.^[172,173]

5.2. Thermosensitive Hydrogels for Capacitive Deionization

CDI is a potential desalination technology in which brackish water flows between two electrodes separated by a spacer, as can be seen in the simplified scheme of Figure 16.^[174]

A CDI cycle consists of two steps. First, the purification of water is conducted by ion electrosorption, where ions are immobilized in porous carbon electrode pairs. In the last step, the absorbed ions, which are released from the electrodes, and are regenerated to repeat the two-step cycle process. CDI can operate at low pressure (sub-osmotic) in comparison to RO and FO systems and, usually, no membrane components are

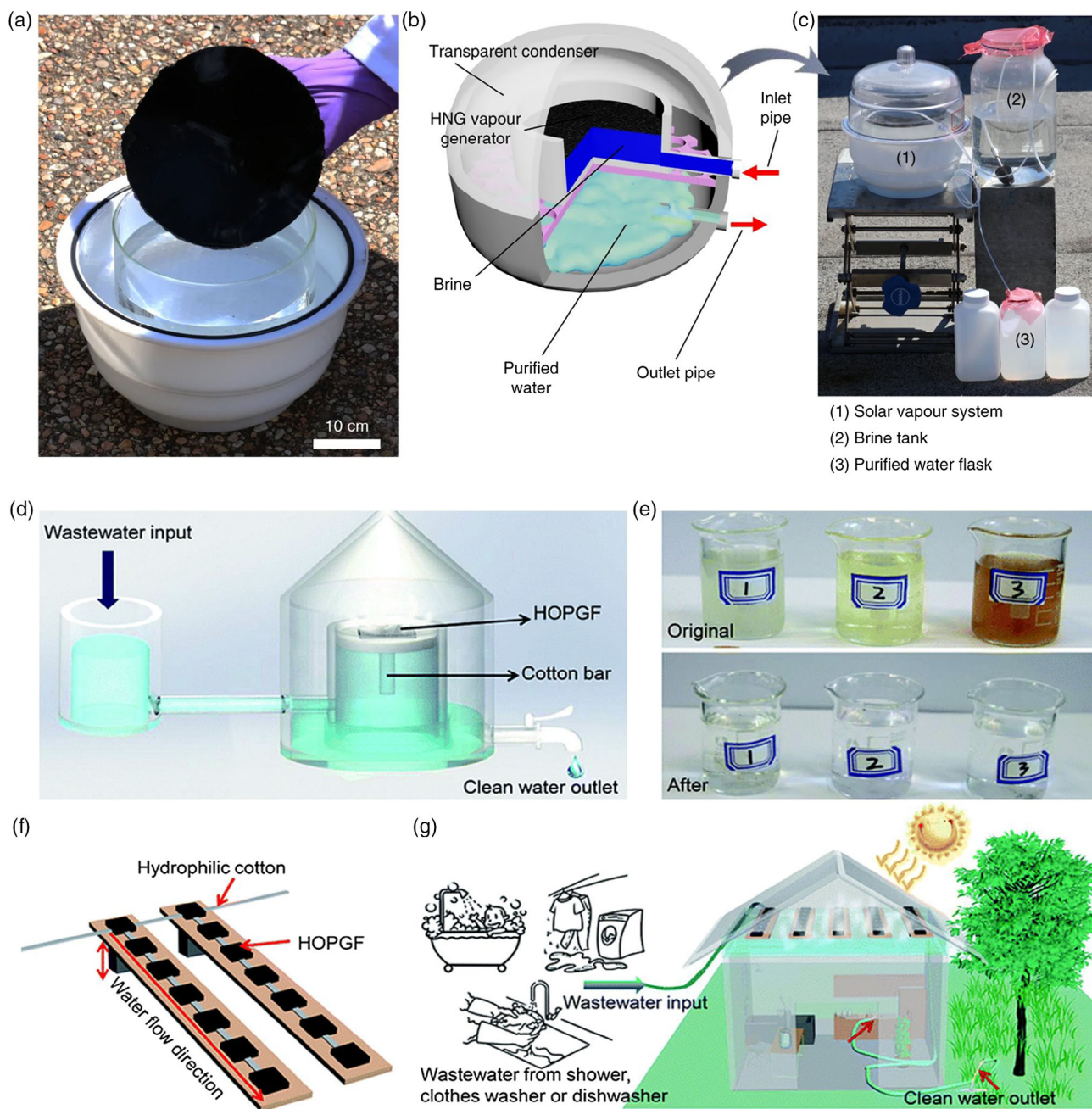


Figure 15. a) Illustration of an outdoor solar water purification membrane using hierarchically nanostructured gel (HNG) based on polyvinyl alcohol (PVA) and PPy in natural sunlight; b) PVA/PPy filter assembly inside a desiccator with transparent lid; c) the homemade prototype for water purification from the brine solution. Reproduced with permission.^[161] Copyright 2018, Springer Nature. d) Scheme of water purification using a vertical system for water collection after evaporation and condensation (HOPGF, highly ordered pillar array structure of graphene framework); e) On top, water contaminated with pharmaceuticals; on bottom, purified water after process of HOPGF and 1 sun; f) Illustration of two pillar array structures with a sequence of 7 PVA/PPy/GO hydrogel; g) solar water purification based on HOPGF under natural sunlight. Reproduced with permission.^[169] Copyright 2018, Royal Society of Chemistry.

required.^[175] Furthermore, energy recovery is also possible since the energy release during electrode regeneration can be used to charge a neighboring cell operating in the first ion electrosorption step.

The CDI efficiency is heavily related to the design of the electrodes and electrode structure. Indeed, the development of

electrodes with a high surface area, good conductivity, and well-controlled Faradaic reactions has attracted most of the recent CDI research.^[176] Nanostructured high-surface carbon materials (i.e., carbon aerogels, activated carbon cloth and fibers, CNTs, carbon nanofibers, and ordered mesoporous carbons) are usually addressed as CDI electrode materials.^[177]

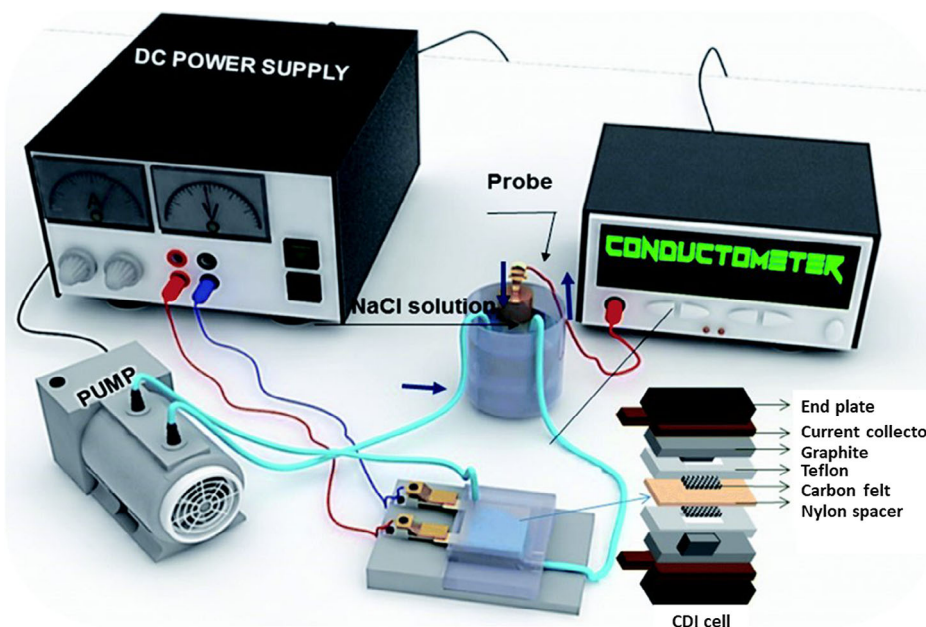


Figure 16. Illustration of CDI cell and the assembly of the equipment used to control the flow (pump), the conductivity of the electrolyte (conductimeter), and to monitor the current applied (potentiostat). Reproduced with permission.^[174] Copyright 2018, Royal Society of Chemistry.

In recent years, hybrid CPHs have been proposed as an alternative to replace carbon-based electrodes for water desalination. The main advantage of hybrid hydrogels is the capability to absorb an immense amount of water, up to several thousand percent of their dry weight, with a high surface exposition to the solution.^[12] The incorporation of CPs has contributed to enhance the pseudo-capacitance and electrosorption of the novel hybrid CDI electrodes due to the good electrical and ions transport properties of such materials. Therefore, CPHs are perfect candidates for CDI systems. The good storage of electrical charges of biodegradable hydrogels modified with conducting polymers to be used as organically modified electrodes in studies related to batteries and supercapacitors have been shown by ours.^[18,178,179] The design of electrodes based on CPHs allows to adjust the intrinsic pore structure, improving the surface properties by increasing the affinity to some metal ions by chelation or redox reactions, and to adjust both the wettability and the zeta potential.^[177]

Pristine graphene hydrogel^[180] (GH) and holey graphene hydrogel^[181] (HGH) were recently proposed as a new electrode material in CDI due to their specific surface, high conductivity, and high hydrophilicity. Moreover, new enhanced composites based on GH and HGH have been proposed by adding conductive additives such as single and multi-walled carbon nanotubes (SWCNTs and MWCNTs),^[182] hollow N-doped mesoporous carbon spheres,^[183] ZrO₂-doped TiO₂ nanofibers,^[184] and ZnO nanoparticles.^[185] Regarding the use of CPs, there are a few examples of CDI technology. Yan et al.^[182] reported the preparation of CDI electrodes made of SWCNTs dispersed in polyaniline (PAni) matrix, while Gu et al.^[186] combined graphene, PPy, and manganese (Mn), as a new composite material to increase CDI performance. In the latter, the CP was loaded into GH and acted

as a “spacer” between graphene sheets, improving the capacitive properties and ion transportation of the composite.

Some of the advantages that might present the CPHs fabricated with TSHs and CPs to move ions from the saltwater to the bulk system are: high porosity, large absorbability, thermal response, capacitive behavior, moderate to high conductivity, and thermal stability. Such properties are fixed by the hydrogel matrix and the capacitive response of the CP units.

Altogether, this makes it a novel and encouraging field of development for novel CDI electrodes made of CPHs with thermal modulation.

6. Summary and Perspective

The present review compiles the most relevant published works related to PNIPAAm thermoresponsive hydrogel and derivatives, on the progress of the past ten years, with respect to their applications in chemical engineering and material science fields. With the advent of “smart” TSH systems and combinations of them with advanced materials, in the future, the development of prototypes based on such hydrogels will gain force due to their superior properties when combined together.

The most promising systems in the biomedical sector seem to be that which combines TSHs with metallic nanoparticles (crystalline structure) and conducting organic materials (covalent structure), i.e., hybrid TSHs, in noninvasive and semi-invasive medical diagnosis, in on-demand bacteria elimination and in drug administration.

In the chemical engineering sector, perhaps the revolution belongs from the use of TSHs to water recovery for self-consumption of the population in areas with water stress, with

water capture induced by sun light. For it, the supply of a water quality fast screening kit to quantify water purity would be necessary, as well as a procedure to recover or purify the hydrogel and the tools, used to manufacture the water collector device, after their uses. The employment of synthetic TSHs in combination with natural hydrogels forecasts to be enhanced in the next years, not only in membrane fabrication for obtaining fresh water, but also in the design of prototypes for metal recovery. In this sense, PNIPAAm hydrogel will play a relevant role due to its modulated LCST property when copolymerized with other acrylamide units, and taking the advantage of its swelling–de-swelling states. Very recently, Park and Lee^[187] reported the purification of water contaminated with Li⁺, promoted by the hydrophilic–hydrophobic transition of PNIPAAm/ALG composite doped with Al³⁺ ions (i.e., playing with its cloud temperature). Tang et al.^[188] were also able to recover UO₂²⁺ from seawater by employing a sodium ALG/PNIPAAm thermoresponsive hydrogel system. Therefore, this TSH application is coming into force.

Unfortunately, in the biomedical area, in vivo assays are scarce. More investigations will be necessary if such “smart” TSHs are intended for implants and/or injection into the human body. In the field of CDI, more investigations will be necessary on materials able to increase the efficiency of water production with respect to energy consumption and electrodes recovery.

Acknowledgements

Grant PID2021-125257OB-I00 funded by MCIN/AEI/10.13039/501100011033 and, by ERDF “A way of making Europe”, by the European Union. Agència de Gestió d'Ajuts Universitaris i de Recerca-AGAUR (2017SGR359) is also acknowledged for financial support to J.M. (Ph.D. fellowship no. 2021 FI SDUR 2017SGR 00359).

Conflict of Interest

The authors declare no conflict of interest.

Keywords

biomedical sensors, poly(*N*-isopropylacrylamide), thermosensitive hydrogels, water cleaning

Received: September 8, 2022

Revised: November 3, 2022

Published online: January 8, 2023

- [1] S. Rimmer, in *Biomedical Hydrogels: Biochemistry, Manufacture and Medical Applications*, Woodhead Publishing, Swaston, Cambridge 2011.
- [2] P. Zarrintaj, M. Jouyandeh, M. R. Ganjali, B. S. Hadavand, M. Mozafari, S. S. Sheiko, M. Vatankeh-Varnoosfaderani, T. J. Gutiérrez, M. R. Saeb, *Eur. Polym. J.* **2019**, *117*, 402.
- [3] H. M. El-Husseiny, E. A. Mady, L. Hamabe, A. Abugomaa, K. Shimada, T. Yoshida, T. Tanaka, A. Yokoi, M. Elbadawy, R. Tanaka, *Mater. Today Bio* **2022**, *13*, 100186.

- [4] S. Soleymani Eil Bakhtiari, H. R. Bakhsheshi-Rad, S. Karbasi, M. Razzaghi, M. Tavakoli, A. F. Ismail, S. Sharif, S. RamaKrishna, X. Chen, F. Berto, *Adv. Eng. Mater.* **2021**, *23*, 2100477.
- [5] G. Ross, S. Ross, B. J. Tighe, in *Brydson's Plast, Mater.* 8th ed. (Ed: M. Gilbert), Elsevier Inc., Amsterdam **2017**, p. 631.
- [6] D. Roy, W. L. A. Brooks, B. S. Sumerlin, *Chem. Soc. Rev.* **2013**, *42*, 7214.
- [7] E. S. Gil, S. M. Hudson, *Prog. Polym. Sci.* **2004**, *29*, 1173.
- [8] Q. Chai, Y. Jiao, X. Yu, *Gels* **2017**, *3*, 6.
- [9] J. A. McCune, S. Mommer, C. C. Parkins, O. A. Scherman, *Adv. Mater.* **2020**, *32*, 1906890.
- [10] S. Lanzalaco, E. Armelin, *Gels* **2017**, *3*, 36.
- [11] J. F. Mano, *Adv. Eng. Mater.* **2008**, *10*, 515.
- [12] A. A. Salehi, M. Ghannadi-Maragheh, M. Torab-Mostaedi, R. Torkaman, M. Asadollahzadeh, *Sep. Purif. Rev.* **2020**, *50*, 380.
- [13] S. W. Sharshir, A. M. Algazzar, K. A. Elmaadawy, A. W. Kandeal, M. R. Elkadeem, T. Arunkumar, J. Zang, N. Yang, *Desalination* **2020**, *491*, 114564.
- [14] R. Colciaghi, R. Simonetti, L. Molinaroli, M. Binotti, G. Manzolini, *Desalination* **2021**, *519*, 115311.
- [15] K. Zhang, F. Li, Y. Wu, L. Feng, L. Zhang, *Desalination* **2020**, *495*, 114667.
- [16] D. Zhao, P. Wang, Q. Zhao, N. Chen, X. Lu, *Desalination* **2014**, *348*, 26.
- [17] Y. Guo, Z. Fang, G. Yu, *Polym. Int.* **2021**, *70*, 1425.
- [18] M. G. Saborío, P. Svelic, J. Casanovas, G. Ruano, M. M. Pérez-Madrugal, L. Franco, J. Torras, F. Estrany, C. Alemán, *Eur. Polym. J.* **2019**, *118*, 347.
- [19] M. M. Pérez-Madrugal, F. Estrany, E. Armelin, D. D. Díaz, C. Alemán, *J. Mater. Chem. A* **2016**, *4*, 1792.
- [20] G. Ruano, J. I. Iribarren, M. M. Pérez-Madrugal, J. Torras, C. Alemán, *Polymers (Basel)*. **2021**, *13*, 1.
- [21] E. Larrañeta, S. Stewart, M. Ervine, R. Al-Kasasbeh, R. Donnelly, *J. Funct. Biomater.* **2018**, *9*, 13.
- [22] D. Lombardo, M. A. Kiselev, M. T. Caccamo, *J. Nanomater.* **2019**, *2019*, 1.
- [23] M. T. Cook, P. Haddow, S. B. Kirton, W. J. McAuley, *Adv. Funct. Mater.* **2021**, *31*, 2008123.
- [24] D. Y. Fan, Y. Tian, Z. J. Liu, *Front. Chem.* **2019**, *7*, 1.
- [25] L. C. S. Erthal, O. L. Gobbo, E. Ruiz-Hernandez, *Acta Biomater.* **2021**, *121*, 89.
- [26] A. Janani, R. Sridhar Skylab, *Int. J. ChemTech Res.* **2014**, *6*, 2233.
- [27] S. Mantha, S. Pillai, P. Khayambashi, A. Upadhyay, Y. Zhang, *Materials* **2019**, *12*, 3323.
- [28] E. Khadem, M. Kharaziha, H. R. Bakhsheshi-Rad, O. Das, F. Berto, *Polymers* **2022**, *14*, 1709.
- [29] S. Chatterjee, P. Hui, C. Kan, *Polymers* **2018**, *10*, 480.
- [30] K. Zubik, P. Singhsa, Y. Wang, H. Manuspiya, R. Narain, *Polymers* **2017**, *9*, 119.
- [31] K. Yang, Q. Han, B. Chen, Y. Zheng, K. Zhang, Q. Li, J. Wang, *Int. J. Nanomed.* **2018**, *13*, 2217.
- [32] S. Li, S. Dong, W. Xu, S. Tu, L. Yan, C. Zhao, J. Ding, X. Chen, *Adv. Sci.* **2018**, *5*, 1700527.
- [33] Y.-Q. Feng, M.-L. Lv, M. Yang, W.-X. Ma, G. Zhang, Y.-Z. Yu, Y.-Q. Wu, H.-B. Li, D.-Z. Liu, Y.-S. Yang, *Molecules* **2022**, *27*, 1638.
- [34] M. Rizwan, S. Rubina Gilani, A. Iqbal Durani, S. Naseem, *J. Adv. Res.* **2021**, *33*, 15.
- [35] K. Ahmed, M. N. I. Shiblee, A. Khosla, L. Nagahara, T. Thundath, H. Furukawa, *J. Electrochem. Soc.* **2020**, *167*, 037563.
- [36] S. Agarwal, S. Jiang, Y. Chen, *Macromol. Mater. Eng.* **2019**, *304*, 1800548.
- [37] O. Wichterle, D. Lim, *Nature* **1960**, *185*, 117.

- [38] E. Armelin, M. M. Pérez-Madriral, C. Alemán, D. D. Díaz, *J. Mater. Chem. A* **2016**, *4*, 8952.
- [39] F. Lin, X. Lu, Z. Wang, Q. Lu, G. Lin, B. Lu, *Cellulose* **2019**, *26*, 1825.
- [40] H. Huang, X. Qi, Y. Chen, Z. Wu, *Saudi Pharm. J.* **2019**, *27*, 990.
- [41] S. Mura, J. Nicolas, P. Couvreur, *Nat. Mater.* **2013**, *12*, 991.
- [42] V. M. Shah, D. X. Nguyen, D. A. Rao, R. G. Alany, A. W. G. Alani, *Temp. Polym.* **2018**, 313.
- [43] M. R. Matanović, J. Kristl, P. A. Grabnar, *Int. J. Pharm.* **2014**, *472*, 262.
- [44] P. Kumar, Y. E. Choonara, V. Pillay, in *Polymer Gels*, Springer, Singapore **2018**, p. 341–359.
- [45] P. Rahmanian-Devin, V. Baradaran Rahimi, V. R. Askari, *Adv. Pharmacol. Pharm. Sci.* **2021**, *8*, 312.
- [46] A. Chenite, M. Buschmann, D. Wang, C. Chaput, N. Kandani, *Carbohydr. Polym.* **2001**, *46*, 39.
- [47] S. Supper, N. Anton, N. Seidel, M. Riemenschnitter, C. Schoch, T. Vandamme, *Langmuir* **2013**, *29*, 10229.
- [48] L. Liu, Q. Gao, X. Lu, H. Zhou, *Asian J. Pharm. Sci.* **2016**, *11*, 673.
- [49] J. S. Barbosa, A. Ribeiro, A. M. Testera, M. Alonso, F. J. Arias, J. C. Rodríguez-Cabello, J. F. Mano, *Adv. Eng. Mater.* **2010**, *12*, B37.
- [50] K. Song, L. Li, X. Yan, W. Zhang, Y. Zhang, Y. Wang, T. Liu, *Mater. Sci. Eng. C* **2017**, *70*, 231.
- [51] Z. Luo, K. Xue, X. Zhang, J. Y. C. Lim, X. Lai, D. J. Young, Z.-X. Zhang, Y.-L. Wu, X. J. Loh, *Biomater. Sci.* **2020**, *8*, 1364.
- [52] U. Adhikari, A. Goliaei, L. Tsereteli, M. L. Berkowitz, *J. Phys. Chem. B* **2016**, *120*, 5823.
- [53] M. A. Abou-Shamat, J. Calvo-Castro, J. L. Stair, M. T. Cook, *Macromol. Chem. Phys.* **2019**, *220*, 1900173.
- [54] S. I. H. Abdi, J. Y. Choi, J. S. Lee, H. J. Lim, C. Lee, J. Kim, H. Y. Chung, J. O. Lim, *Tissue Eng. Regen. Med.* **2012**, *9*, 1.
- [55] B. K. Lau, Q. Wang, W. Sun, L. Li, *J. Polym. Sci. Part B Polym. Phys.* **2004**, *42*, 2014.
- [56] J. M. White, M. A. Calabrese, *Colloids Surfaces A Physicochem. Eng. Asp.* **2022**, *638*, 128246.
- [57] A. S. L. Rangabhatla, V. Tantishaiyakul, K. Oungbho, O. Boonrat, *Int. J. Pharm.* **2016**, *499*, 110.
- [58] S. P. Quah, A. J. Smith, A. N. Preston, S. T. Laughlin, S. R. Bhatia, *Polymer (Guildf)*. **2018**, *135*, 171.
- [59] S. C. Barros, A. A. da Silva, D. B. Costa, I. Cesarino, C. M. Costa, S. Lanceros-Méndez, A. Pawlicka, M. M. Silva, *Cellulose* **2014**, *21*, 4531.
- [60] R. Wang, X. Yao, T. Li, X. Li, M. Jin, Y. Ni, W. Yuan, X. Xie, L. Lu, M. Li, *Adv. Healthc. Mater.* **2019**, *8*, 1900967.
- [61] B. Niemczyk-Soczynska, A. Gradyś, D. Kolbuk, A. Krzton-Maziopa, P. Sajkiewicz, *Polymers* **2019**, *11*, 1772.
- [62] Y. I. Wang, S. Zhang, J. Lee, *Theory Pract. Log. Program.* **2019**, *19*, 1090.
- [63] W. Huang, R. Ramesh, P. K. Jha, R. G. Larson, *Macromolecules* **2016**, *49*, 1490.
- [64] V. Hynninen, S. Hietala, J. R. McKee, L. Murtoimäki, O. J. Rojas, O. Ikkala, N. Nonappa, *Biomacromolecules* **2018**, *19*, 2795.
- [65] B. Gaihe, J. M. Unagolla, J. Liu, N. A. Ebraheim, A. C. Jayasuriya, *ACS Biomater. Sci. Eng.* **2019**, *5*, 4587.
- [66] K. Brewer, B. Gundsambuu, P. F. Marina, S. C. Barry, A. Blencowe, *Polymers* **2020**, *12*, 367.
- [67] K. Zhang, K. Xue, X. J. Loh, *Gels* **2021**, *7*, 77.
- [68] K. Xue, X. Zhao, Z. Zhang, B. Qiu, Q. S. W. Tan, K. H. Ong, Z. Liu, B. H. Parikh, V. A. Barathi, W. Yu, X. Wang, G. Lingam, W. Hunziker, X. Su, X. J. Loh, *Biomater. Sci.* **2019**, *7*, 4603.
- [69] F. Oroojalian, M. Babaei, S. M. Taghdisi, K. Abnous, M. Ramezani, M. Alibolandi, *J. Control. Release* **2018**, *288*, 45.
- [70] P. Shang, J. Wu, X. Shi, Z. Wang, F. Song, S. Liu, *Polymers* **2019**, *11*.
- [71] X. Z. Zhang, R. X. Zhuo, *Eur. Polym. J.* **2000**, *36*, 643.
- [72] M. Heskins, J. E. Guillet, *J. Macromol. Sci. Part A Chem.* **1968**, *2*, 1441.
- [73] J. Wang, Q. Zhong, J. Wu, T. Chen, in *Handb. Smart Text.* (Ed: X. Tao), Springer Singapore **2015**, 919.
- [74] T. Buchecker, P. Schmid, I. Grillo, S. Prévost, M. Drechsler, O. Diat, A. Pfitzner, P. Bauduin, *J. Am. Chem. Soc.* **2019**, *141*, 6890.
- [75] L. Tavagnacco, E. Zaccarelli, E. Chiessi, *Phys. Chem. Chem. Phys.* **2018**, *20*, 9997.
- [76] M. S. Liu, C. Taylor, B. Chong, L. Liu, A. Bilic, N. S. Terefe, R. Stockmann, S. H. Thang, K. De Silva, *Eur. Polym. J.* **2014**, *55*, 153.
- [77] M. M. Rana, A. Rajeev, G. Natale, H. De la Hoz Siegler, *J. Mater. Res. Technol.* **2021**, *13*, 769.
- [78] R. A. Stile, W. R. Burghardt, K. E. Healy, *Macromolecules* **1999**, *32*, 7370.
- [79] M. Najafi, E. Hebels, W. E. Hennink, T. Vermonden, in *Temp-Resp. Polym. Chem. Prop. Appl.* (Eds: V. V. Khutoryanskiy, T.K. Georgiou), John Wiley & Sons, Inc., Hoboken, NJ **2018**, p. 3–34, Chap. 1.
- [80] M. Ziminska, J. J. Wilson, E. McErlean, N. Dunne, H. O. McCarthy, *Materials* **2020**, *13*, 2530.
- [81] M. Teodorescu, K. Matyjaszewski, *Macromolecules* **1999**, *32*, 4826.
- [82] M. Teodorescu, K. Matyjaszewski, *Macromol. Rapid Commun.* **2000**, *21*, 190.
- [83] Z. M. O. Rzaev, S. Dinger, E. Pişkin, *Prog. Polym. Sci.* **2007**, *32*, 534.
- [84] X. Yin, A. S. Hoffman, P. S. Stayton, *Biomacromolecules* **2006**, *7*, 1381.
- [85] R. Shimura, Y. Suematsu, H. Horiuchi, S. Takeoka, A. Oshima, M. Washio, *Radiat. Phys. Chem.* **2020**, *171*, 108741.
- [86] M. M. S. Lencina, C. Rizzo, C. Demitri, N. Andreucetti, A. Maffezzoli, *Radiat. Phys. Chem.* **2019**, *156*, 38.
- [87] S. Lanzalaco, P. Turon, C. Weis, C. Alemán, E. Armelin, *Soft Matter* **2019**, *15*, 3432.
- [88] S. Lanzalaco, L. J. Del Valle, P. Turon, C. Weis, F. Estrany, C. Alemán, E. Armelin, *J. Mater. Chem. B* **2020**, *8*, 1049.
- [89] S. Lanzalaco, P. Turon, C. Weis, C. Mata, E. Planas, C. Alemán, E. Armelin, *Adv. Funct. Mater.* **2020**, 2004145.
- [90] Y. G. Takei, T. Aoki, K. Sanui, N. Ogata, T. Okano, Y. Sakurai, *Bioconjug. Chem.* **1993**, *4*, 341.
- [91] T. Baltes, F. Garret-Flaudy, R. Freitag, *J. Polym. Sci. Part A Polym. Chem.* **1999**, *37*, 2977.
- [92] H. G. Schild, D. A. Tirrell, *J. Phys. Chem.* **1990**, *94*, 4352.
- [93] S. Furry, Y. Zhang, D. Ortiz-Acosta, P. S. Cremer, D. E. Bergbreiter, *J. Polym. Sci. Part A Polym. Chem.* **2006**, *44*, 1492.
- [94] K. Van Durme, G. Van Assche, B. Van Mele, *Macromolecules* **2004**, *37*, 9596.
- [95] F. Afroze, E. Nies, H. Berghmans, *J. Mol. Struct.* **2000**, *554*, 55.
- [96] X. Zhang, R. Zhuo, *J. Colloid Interface Sci.* **2000**, *223*, 311.
- [97] H. Feil, Y. H. Bae, J. Feijen, S. W. Kim, *Macromolecules* **1993**, *26*, 2496.
- [98] H. Thérien-Aubin, Z. L. Wu, Z. Nie, E. Kumacheva, *J. Am. Chem. Soc.* **2013**, *135*, 4834.
- [99] T. Takigawa, T. Yamawaki, K. Takahashi, T. Masuda, *Polym. Gels Networks* **1998**, *5*, 585.
- [100] J. T. Lee, J. Lee, Y. Kwon, J. Y. Kim, Y. Lin, Y.-H. Lee, S. R. Paik, *Sensors Actuators B Chem.* **2020**, *305*, 127514.
- [101] Y. Wu, H. Wang, F. Gao, Z. Xu, F. Dai, W. Liu, *Adv. Funct. Mater.* **2018**, *28*, 1801000.
- [102] S. Jiang, K. Wang, Y. Dai, X. Zhang, F. Xia, *Macromol. Mater. Eng.* **2019**, *304*, 1900087.
- [103] B. Mutharani, P. Ranganathan, S. M. Chen, S. K. D. Vishnu, *Sensors Actuators, B Chem.* **2020**, *304*, 127232.

- [104] Y. Zhu, S. Liu, X. Shi, D. Han, F. Liang, *Mater. Chem. Front.* **2018**, 2, 2212.
- [105] C. Qian, T. Higashigaki, T.-A. Asoh, H. Uyama, *ACS Appl. Mater. Interfaces* **2020**, 12, 27518.
- [106] Y. H. Roh, J. Y. Eom, D. G. Choi, J. Y. Moon, M. S. Shim, K. W. Bong, *J. Ind. Eng. Chem.* **2021**, 98, 211.
- [107] I. Matai, G. Kaur, S. Soni, A. Sachdev, **Vikas, S. Mishra, *J. Photochem. Photobiol. B Biol.* **2020**, 210, 111960.
- [108] D. Besold, S. Risse, Y. Lu, J. Dzubiella, M. Ballauff, *Ind. Eng. Chem. Res.* **2021**, 60, 3922.
- [109] Y. Gao, J. Chen, X. Han, Y. Pan, P. Wang, T. Wang, T. Lu, *Adv. Funct. Mater.* **2020**, 30, 2003207.
- [110] J. Yang, R. Bai, B. Chen, Z. Suo, *Adv. Funct. Mater.* **2020**, 30, 1901693.
- [111] K. Arroub, I. Gessner, T. Fischer, S. Mathur, *Adv. Eng. Mater.* **2021**, 23, 2100221.
- [112] L. J. Luo, D. D. Nguyen, J. Y. Lai, *Mater. Sci. Eng. C* **2020**, 115, 111095.
- [113] M. Zhu, J. Wang, N. Li, *Artif. Cells, Nanomed. Biotechnol.* **2018**, 46, 1282.
- [114] Z. Lu, Z. Zhang, Y. Tang, *ACS Appl. Bio Mater.* **2019**, 2, 4485.
- [115] S. L. Banerjee, S. Das, K. Bhattacharya, M. Kundu, M. Mandal, N. K. Singha, *Chem. Eng. J.* **2021**, 405, 126436.
- [116] X. Han, R. Yang, X. Wan, J. Dou, J. Yuan, B. Chi, J. Shen, *J. Mater. Chem. B* **2021**, 9, 6212.
- [117] M. Nizioł, J. Paleczny, A. Junka, A. Shavandi, A. Dawiec-Liśniewska, D. Podstawczyk, *Bioengineering* **2021**, 8, 79.
- [118] S. O. Blacklow, J. Li, B. R. Freedman, M. Zeidi, C. Chen, D. J. Mooney, *Sci. Adv.* **2019**, 5, 1.
- [119] K. Nagase, T. Okano, *J. Mater. Chem. B* **2016**, 4, 6381.
- [120] K. Nagase, Y. Hatakeyama, T. Shimizu, K. Matsuura, M. Yamato, N. Takeda, T. Okano, *Biomacromolecules* **2015**, 16, 532.
- [121] K. Nagase, M. Yamato, H. Kanazawa, T. Okano, *Biomaterials* **2018**, 153, 27.
- [122] Y. Maekawa, E. Ayano, K. Nagase, H. Kanazawa, *Anal. Sci.* **2021**, 37, 651.
- [123] K. Nagase, M. Shimura, R. Shimane, K. Hanaya, S. Yamada, A. M. Akimoto, T. Sugai, H. Kanazawa, *Biomater. Sci.* **2021**, 9, 663.
- [124] M. Barsbay, O. Güven, *Eur. Polym. J.* **2021**, 147, 110330.
- [125] M. Nakayama, T. Kanno, H. Takahashi, A. Kikuchi, M. Yamato, T. Okano, *Sci. Technol. Adv. Mater.* **2021**, 22, 481.
- [126] R. Quidant, S. Santos, P. Turon, S. Thomson, C. Weis, I. Martínez, US Patent, US2016227786A1, **2016**.
- [127] I. De Miguel, I. Prieto, A. Albornoz, V. Sanz, C. Weis, P. Turon, R. Quidant, *Nano Lett.* **2019**, 19, 2524.
- [128] E. Lenzi, D. Jimenez De Aberasturi, L. M. Liz-Marzán, *ACS Sensors* **2019**, 4, 1126.
- [129] R. A. Álvarez-Puebla, R. Contreras-Cáceres, I. Pastoriza-Santos, J. Pérez-Juste, L. M. Liz-Marzán, *Angew. Chem. Int. Ed.* **2009**, 48, 138.
- [130] G. Bodelón, V. Montes-García, C. Fernández-López, I. Pastoriza-Santos, J. Pérez-Juste, L. M. Liz-Marzán, *Small* **2015**, 11, 4149.
- [131] N. H. Ly, S.-W. Joo, *J. Mater. Chem. B* **2020**, 8, 186.
- [132] S. E. Bohndiek, A. Wagadarikar, C. L. Zavaleta, D. Van De Sompel, E. Garai, J. V. Jokerst, S. Yazdanfar, S. S. Gambhir, *Proc. Natl. Acad. Sci. USA* **2013**, 110, 12408.
- [133] S. Lanzalaco, P. Gil, J. Mingot, A. Águeda, C. Alemán, E. Armelin, *ACS Biomater. Sci. Eng.* **2022**, 8, 3329.
- [134] D. Franke, S. Binder, G. Gerlach, *IEEE Sensors Lett.* **2017**, 1, 1.
- [135] D. Franke, G. Gerlach, *J. Sensors Sens. Syst.* **2021**, 10, 93.
- [136] C. Y. Lo, Y. Zhao, C. Kim, Y. Alsaid, R. Khodambashi, M. Peet, R. Fisher, H. Marvi, S. Berman, D. Aukes, X. He, *Mater. Today* **2021**, 50, 35.
- [137] Z. Wang, H. Zhou, W. Chen, Q. Li, B. Yan, X. Jin, A. Ma, H. Liu, W. Zhao, *ACS Appl. Mater. Interfaces* **2018**, 10, 14045.
- [138] O. Y. Kweon, S. K. Samanta, Y. Won, J. H. Yoo, J. H. Oh, *ACS Appl. Mater. Interfaces* **2019**, 11, 26134.
- [139] J. Yan, Y. Xia, J. Lai, C. Zhao, D. Xiang, H. Li, Y. Wu, Z. Li, H. Zhou, *Macromol. Mater. Eng.* **2022**, 307, 2100765.
- [140] M. Nakamitsu, H. Imai, Y. Oaki, *ACS Sensors* **2020**, 5, 133.
- [141] A. I. Robby, G. Lee, S. Y. Park, *Sensors Actuators B Chem.* **2019**, 297, 126783.
- [142] Y. Wei, Q. Zeng, M. Wang, J. Huang, X. Guo, L. Wang, *Biosens. Bioelectron.* **2019**, 131, 156.
- [143] Y. Jiang, M. G. Colazo, M. J. Serpe, *Colloid Polym. Sci.* **2016**, 294, 1733.
- [144] I. Thivaos, V. Koukountzis, J. K. Kallitsis, G. Bokias, *Sensors Actuators, B Chem.* **2016**, 233, 127.
- [145] P. Zhao, M. Ni, C. Chen, Z. Zhou, X. Li, C. Li, Y. Xie, J. Fei, *Nanoscale* **2019**, 11, 7394.
- [146] B. Mutharani, P. Ranganathan, S.-M. Chen, *Sensors Actuators B Chem.* **2020**, 304, 127361.
- [147] B. Mutharani, T.-W. Chen, S.-M. Chen, X. Liu, *Sensors Actuators B Chem.* **2020**, 316, 128103.
- [148] S. M. Mugo, Dhanjai, J. Alberkant, *IEEE Sens. J.* **2020**, 20, 5741.
- [149] J. Huang, M. Li, P. Zhang, P. Zhang, L. Ding, *Sensors Actuators, B Chem.* **2016**, 237, 24.
- [150] X. Dan, L. Ruiyi, W. Qinsheng, Y. Yongqiang, W. Guangli, L. Zaijun, *Microchem. J.* **2022**, 172, 2.
- [151] X. Li, M. J. Serpe, *Adv. Funct. Mater.* **2016**, 26, 3282.
- [152] J. E. Lee, K. Chung, J. Lee, K. Shin, D. H. Kim, *Adv. Funct. Mater.* **2015**, 25, 6716.
- [153] A. C. Manikas, A. Aliberti, F. Causa, E. Battista, P. A. Netti, *J. Mater. Chem. B* **2015**, 3, 53.
- [154] Y. Cozzens, D. M. Steeves, J. W. Soares, J. E. Whitten, *Macromolecules* **2019**, 52, 2900.
- [155] S. Nie, Z. Li, Y. Yao, Y. Jin, *Front. Chem.* **2021**, 9, 1137.
- [156] H. He, L. Zhang, X. Guan, H. Cheng, X. Liu, S. Yu, J. Wei, J. Ouyang, *ACS Appl. Mater. Interfaces* **2019**, 11, 26185.
- [157] G. Fabregat, B. Teixeira-Dias, L. J. del Valle, E. Armelin, F. Estrany, C. Alemán, *ACS Appl. Mater. Interfaces* **2014**, 6, 11940.
- [158] X. Fan, W. Nie, H. Tsai, N. Wang, H. Huang, Y. Cheng, R. Wen, L. Ma, F. Yan, Y. Xia, *Adv. Sci.* **2019**, 6, 1900813.
- [159] I. Babeli, G. Ruano, J. Casanovas, M.-P. Ginebra, J. García-Torres, C. Alemán, *J. Mater. Chem. C* **2020**, 8, 8654.
- [160] K. M. Shah, I. H. Billinge, X. Chen, H. Fan, Y. Huang, R. K. Winton, N. Y. Yip, *Desalination* **2022**, 538, 115827.
- [161] F. Zhao, X. Zhou, Y. Shi, X. Qian, M. Alexander, X. Zhao, S. Mendez, R. Yang, L. Qu, G. Yu, *Nat. Nanotechnol.* **2018**, 13, 489.
- [162] X. Zhou, Y. Guo, F. Zhao, G. Yu, *Acc. Chem. Res.* **2019**, 52, 3244.
- [163] Y. Guo, G. Yu, *Accounts Mater. Res.* **2021**, 2, 374.
- [164] P. Zhang, F. Liu, Q. Liao, H. Yao, H. Geng, H. Cheng, C. Li, L. Qu, *Angew. Chem.* **2018**, 130, 16581.
- [165] H. Geng, Q. Xu, M. Wu, H. Ma, P. Zhang, T. Gao, L. Qu, T. Ma, C. Li, *Nat. Commun.* **2019**, 10, 1512.
- [166] L. Zang, C. Finnerty, S. Zheng, K. Conway, L. Sun, J. Ma, B. Mi, *Water Res.* **2021**, 198, 117135.
- [167] X. Zhou, F. Zhao, Y. Guo, B. Rosenberger, G. Yu, *Sci. Adv.* **2019**, 5, 1.
- [168] F. Zhao, X. Zhou, Y. Liu, Y. Shi, Y. Dai, G. Yu, *Adv. Mater.* **2019**, 31.
- [169] P. Zhang, Q. Liao, H. Yao, H. Cheng, Y. Huang, C. Yang, L. Jiang, L. Qu, *J. Mater. Chem. A* **2018**, 6, 15303.
- [170] M. A. Anderson, A. L. Cudero, J. Palma, *Electrochim. Acta* **2010**, 55, 3845.
- [171] A. Subramani, J. G. Jacangelo, *Water Res.* **2015**, 75, 164.

- [172] S. Porada, R. Zhao, A. Van Der Wal, V. Presser, P. M. Biesheuvel, *Prog. Mater. Sci.* **2013**, *58*, 1388.
- [173] F. A. AlMarzooqi, A. A. Al Ghaferi, I. Saadat, N. Hilal, *Desalination* **2014**, *342*, 3.
- [174] S. K. Sami, J. Y. Seo, S. E. Hyeon, M. S. A. Shershah, P. J. Yoo, C. H. Chung, *RSC Adv.* **2018**, *8*, 4182.
- [175] E. Avraham, M. Noked, A. Soffer, D. Aurbach, *Electrochim. Acta* **2011**, *56*, 6312.
- [176] T. Humplik, J. Lee, S. C. O'Hern, B. A. Fellman, M. A. Baig, S. F. Hassan, M. A. Atieh, F. Rahman, T. Laoui, R. Karnik, E. N. Wang, *Nanotechnology* **2011**, *22*, 292001.
- [177] Y. Liu, C. Nie, X. Liu, X. Xu, Z. Sun, L. Pan, *RSC Adv.* **2015**, *5*, 15205.
- [178] M. M. Pérez-Madrugal, M. G. Edo, M. G. Saborío, F. Estrany, C. Alemán, *Carbohydr. Polym.* **2018**, *200*, 456.
- [179] B. G. Molina, A. Llampayas, G. Fabregat, F. Estrany, C. Alemán, J. Torras, *J. Appl. Polym. Sci.* **2021**, *138*, 50062.
- [180] J. Ma, L. Wang, F. Yu, *Electrochim. Acta* **2018**, *263*, 40.
- [181] J. Cao, Y. Wang, C. Chen, F. Yu, J. Ma, *J. Colloid Interface Sci.* **2018**, *518*, 69.
- [182] C. Yan, L. Zou, R. Short, *Desalination* **2012**, *290*, 125.
- [183] M. Mi, X. Liu, W. Kong, Y. Ge, W. Dang, J. Hu, *Desalination* **2019**, *464*, 18.
- [184] A. S. Yasin, A. Y. Mohamed, I. M. A. Mohamed, D. Y. Cho, C. H. Park, C. S. Kim, *Chem. Eng. J.* **2019**, *371*, 166.
- [185] A. S. Yasin, A. Yousef Mohamed, D. H. Kim, T. Luu Luyen Doan, S. S. Chougule, N. Jung, S. Nam, K. Lee, *Sep. Purif. Technol.* **2021**, *277*, 119428.
- [186] X. Gu, Y. Yang, Y. Hu, M. Hu, J. Huang, C. Wang, *J. Mater. Chem. A* **2015**, *3*, 5866.
- [187] S. H. Park, S. J. Lee, *Green Energy Environ.* **2022**, *7*, 334.
- [188] L. Tang, S. Ren, T. Zhang, X. Wei, M. Li, X. Yin, S. Wei, *Chem. Eng. J.* **2021**, *425*, 130589.
- [189] A. Ali, S. Ahmed, *J. Agr. Food Chem.* **2018**, *66*, 6940.
- [190] M. M. Pérez-Madrugal, J. Torras, J. Casanovas, M. Häring, C. Alemán, D. D. Díaz, *Biomacromolecules* **2017**, *18*, 2967.
- [191] E. Armelin, R. Whelan, Y. Martínez-Triana, C. Alemán, M. G. Finn, D. Díaz Díaz, *ACS Appl. Mater. Interfaces* **2017**, *9*, 4231.
- [192] P. Raknam, N. Balekar, R. Teanpaisan, T. Amnuaitik, *J. Oral Microbiol.* **2022**, *14*, 1.
- [193] M. Dhanka, V. Pawar, D. S. Chauhan, N. K. Jain, R. S. Prabhuraj, C. Shetty, M. K. Kumawat, R. Prasad, R. Srivastava, *Colloids Surf. B Biointerfaces* **2021**, *201*, 111597.
- [194] M. Ghanbari, A. Sadjadinia, N. Zahmatkesh, F. Mohandes, B. Dolatyar, B. Zeynali, M. Salavati-Niasari, *Polym. Test.* **2022**, *110*, 107562.
- [195] N. Bhattarai, J. Gunn, M. Zhang, *Adv. Drug Deliv. Rev.* **2010**, *62*, 83.
- [196] M. Anwary, P. Kumar, L. C. du Toit, Y. E. Choonara, V. Pillay, *Artif. Cells, Nanomed. Biotechnol.* **2018**, *46*, 1074.
- [197] A. J. Rocker, M. Cavin, N. R. Johnson, R. Shandas, D. Park, *ACS Biomater. Sci. Eng.* **2022**, *8*, 3883.
- [198] L. Chen, P. S. Doyle, *Adv. Mater.* **2021**, *33*, 2008618.
- [199] Y. Huang, W. Guo, J. Zhang, X. Peng, G. Li, L.-M. Zhang, L. Yang, *Cellulose* **2020**, *27*, 1555.
- [200] Y. Guo, W. Guan, C. Lei, H. Lu, W. Shi, G. Yu, *Nat. Commun.* **2022**, *13*, 2761.
- [201] C. Cai, H. Zhu, Y. Chen, Y. Guo, Z. Yang, H. Li, H. Liu, *ACS Nano* **2022**, <https://doi.org/10.1021/acsnano.2c07483>.
- [202] W. C. Huang, C. C. Lin, T. W. Chiu, S. Y. Chen, *ACS Appl. Mater. Interfaces* **2022**, *14*, 46200.
- [203] E. Kushan, E. Senses, *ACS Appl. Bio Mater.* **2021**, *4*, 3507.
- [204] Q. Lei, L. Wang, H. Xie, W. Yu, *Build. Environ.* **2022**, *222*, 109407.
- [205] H. Zhao, Y. Huang, F. Lv, L. Liu, Q. Gu, S. Wang, *Adv. Funct. Mater.* **2021**, *31*, 2105544.
- [206] M. R. Dethé, P. A. H. Ahmed, M. Agrawal, U. Roy, A. Alexander, *J. Control. Release* **2022**, *343*, 217.
- [207] W. W. M. Soh, J. Zhu, X. Song, D. Jain, E. K. F. Yim, J. Li, *J. Mater. Chem. B* **2022**, *10*, 8407.
- [208] H. Haidari, R. Bright, X. L. Strudwick, S. Garg, K. Vasilev, A. J. Cowin, Z. Kopecki, *Acta Biomater.* **2021**, *128*, 420.
- [209] B. Fan, N. Cui, Z. Xu, K. Chen, P. Yin, K. Yue, W. Tang, *Biomacromolecules* **2022**, *23*, 972.
- [210] S. Fan, Z. Li, C. Fan, J. Chen, H. Huang, G. Chen, S. Liu, H. Zhou, R. Liu, Z. Feng, Y. Zhang, H. Hu, Z. Huang, Y. Qin, J. Liang, *J. Hazard. Mater.* **2022**, *433*, 128808.
- [211] S.-Y. Park, J.-H. Kang, H.-S. Kim, J.-Y. Hwang, U. S. Shin, *Nanoscale* **2022**, *14*, 2367.



Sonia Lanzalaco is a chemical engineer and Ph.D. (from 2016) by the Università degli Studi di Palermo (UniPa, Italy), with research interests mainly focused on materials science and polymer technology. In 2015, she was visiting researcher at Carnegie Mellon University (CMU, USA) under the supervision of world-renowned Prof. Krzysztof Matyjaszewski. In 2017 she moved to Spain and, in 2018, she obtained the prestigious Individual Marie Skłodowska-Curie Fellowship (MSCA), carried out at the IMEM's group at Universitat Politècnica de Catalunya (UPC). Currently, she is a scientific researcher at UPC, under the supervision of Prof. Carlos Alemán and Prof. Elaine Armelin.



Júlia Mingot Béjar studied chemical engineering at Universitat Politècnica de València (UPV, Spain) where she got her bachelor degree in 2017 and continued her master's studies in Universitat Rovira i Virgili (URV, Spain) focusing in nanoscience. In 2022, she started her Ph.D. in polymers and biopolymers field at the Innovation in Materials and Molecular Engineering group (IMEM), at Universitat Politècnica de Catalunya (UPC, Spain). She is currently working with thermosensitive hydrogels and SERS active nanoparticles for applications in biomedical and chemical engineering areas.



Juan Torras is associate professor in the Chemical Engineering Department and the Barcelona Research Center in Multiscale Science and Engineering, Universitat Politècnica de Catalunya (UPC, Spain). He earned his Ph.D. in Chemistry at the Universitat Rovira i Virgili in 1997. His main research interests focus on conducting polymers and biodegradable polymers for biomedical and environmental applications, and the development of new computational tools to model biopolymers.



Carlos Alemán graduated in chemistry from the University of Barcelona (Spain). He received the Ph.D. from the Polytechnic University of Catalonia (UPC) in 1994, where he was promoted to the position of full professor. He was postdoctoral researcher at the ETH and visiting professor at the Università di Napoli Federico II, University of Twente and Universidade Federal do Rio Grande do Sul. Since 2003 he is the leader of the “Innovation in Materials and Molecular Engineering” group. His main research interests focus on polymers for biomedical applications, especially biosensors, energy storage devices and, most recently, the development of electrothermal catalysts.



Elaine Armelin is full professor at Universitat Politècnica de Catalunya (UPC, Spain) and research staff of the Innovation in Materials and Molecular Engineering Group (IMEM). She received her bachelor's degree in chemistry in 1995 and master's degree in organic chemistry in 1997, at Universidade de São Paulo (USP, Brazil). In 1997 she moved to Barcelona to perform her Ph.D. studies in polymer science, at the Department of Chemical Engineering at UPC. Her current work focuses on the developing of functional polymers, sustainable polymers, eco-friendly coatings and adhesives, thermosensitive hydrogels, 3D-printing processes, biodegradation and biocompatibility studies.